



HAL
open science

**Stenopterygiids from the lower Toarcian of Beaujolais
and a chemostratigraphic context for ichthyosaur
preservation during the Toarcian Oceanic Anoxic Event
Running header: Toarcian ichthyosaurs and the T-OAE**

Jérémy Martin, Guillaume Suan, Baptiste Suchéras-Marx, Louis Rulleau, Jan Schlögl, Kevin Janneau, Matt Williams, Alex Léna, Anne-Sabine Grosjean, Estel Sarroca, et al.

► **To cite this version:**

Jérémy Martin, Guillaume Suan, Baptiste Suchéras-Marx, Louis Rulleau, Jan Schlögl, et al.. Stenopterygiids from the lower Toarcian of Beaujolais and a chemostratigraphic context for ichthyosaur preservation during the Toarcian Oceanic Anoxic Event Running header: Toarcian ichthyosaurs and the T-OAE. The Geological Society, London, Special Publications, 2021, 514 (1), pp.153. 10.1144/SP514-2020-232 . hal-03357742

HAL Id: hal-03357742

<https://hal.science/hal-03357742>

Submitted on 29 Sep 2021

HAL is a multi-disciplinary open access archive for the deposit and dissemination of scientific research documents, whether they are published or not. The documents may come from teaching and research institutions in France or abroad, or from public or private research centers.

L'archive ouverte pluridisciplinaire **HAL**, est destinée au dépôt et à la diffusion de documents scientifiques de niveau recherche, publiés ou non, émanant des établissements d'enseignement et de recherche français ou étrangers, des laboratoires publics ou privés.

1 **Stenopterygiids from the lower Toarcian of Beaujolais and a chemostratigraphic**
2 **context for ichthyosaur preservation during the Toarcian Oceanic Anoxic Event**

3
4 Running header: Toarcian ichthyosaurs and the T-OAE

5
6 Jeremy E. Martin^{1*}, Guillaume Suan¹, Baptiste Suchéras-Marx², Louis Rulleau³, Jan
7 Schlögl⁴, Kevin Janneau⁵, Matt Williams⁶, Alex Léna⁷, Anne-Sabine Grosjean⁸, Estel
8 Sarroca⁸, Vincent Perrier¹, Vincent Fernandez⁹, Anne-Lise Charruault¹⁰, Erin E.
9 Maxwell¹¹ and Peggy Vincent¹²

10
11 ¹Université de Lyon, UCBL, ENSL, CNRS, UMR 5276 LGL-TPE, 69622

12 Villeurbanne, France

13 ²Aix Marseille Univ, CNRS, IRD, INRA, Coll France, CEREGE, Aix-en-Provence,

14 France

15 ³169 chemin de l'Herbetan, F-69380 Chasselay, France

16 ⁴Department of Geology and Paleontology, Faculty of Natural Sciences, Comenius
17 University in Bratislava, Mlynská dolina, Ilkovičova 6, 84215 Bratislava, Slovakia

18 ⁵Université de Strasbourg (UNISTRA), Jardin des sciences, 12 rue de l'Université,
19 67000 Strasbourg, France

20 ⁶Bath Royal Literary and Scientific Institution, 16–18 Queen Square, Bath BA1 2HN,

21 UK

22 ⁷Université de Lyon, Université Claude Bernard Lyon 1, S2HEP EA 4148, La Pagode,

23 43 Bd du 11 novembre 1918, 69622 Villeurbanne, France

24 ⁸Paleorhodania, 69006 Lyon - France

25 ⁹Imaging and Analysis Centre, Natural History Museum, Cromwell

26 Road SW7, London 5BD, UK

27 ¹⁰Université de Montpellier, CNRS, IRD, EPHE (UM), Institut des Sciences de

28 l'Evolution de Montpellier, 163 rue Auguste Broussonnet - 34090 Montpellier, France

29 ¹¹Staatliches Museum für Naturkunde Stuttgart, Rosenstein 1, 70191, Stuttgart,

30 Germany

31 ¹²Sorbonne Université (CNRS-MNHN-UPMC) – Muséum national d'Histoire
32 naturelle, Département Origines et Evolution, UMR CNRS-MNHN-UPMC 7207,
33 Centre de Recherche en Paléontologie-Paris (CR2P), 57, rue Cuvier - 75231 Paris

34 Cedex 05, France

35
36
37
38
39
40
41
42
43
44
45
46
47
48
49
50
51
52
53
54
55
56
57
58
59
60
61
62
63
64
65
66
67
68

*Correspondence: (jeremy.martin@ens-lyon.fr)

Keywords: Lower Jurassic, Toarcian Oceanic Anoxic Event, chemostratigraphy, Lagerstätte-type deposits, marine reptiles, Ichthyosauria

Abstract: We report new ichthyosaur material excavated in lower Toarcian levels of the LafargeHolcim Val d’Azergues quarry in Beaujolais, SE France. A partially articulated skull and a smaller, unprepared but likely subcomplete skeleton preserved in a carbonate concretion are identified as stenopterygiids, a family of wide European distribution during the Early Jurassic. These specimens are among the finest preserved Toarcian exemplars known from Europe and in one of them, soft tissue preservation is suspected. Their state of preservation is attributed to the combination of prolonged anoxic conditions near the water-sediment interface and early carbonate cementation resulting from the activity of sulfate-reducing bacteria. We also present carbon and strontium isotope values obtained from the study site that allow detailed temporal comparisons with other Toarcian vertebrate-yielding sites and environmental perturbations associated with the Toarcian Oceanic Anoxic Event (T-OAE). These comparisons suggest that the relatively high abundance and good preservation state of Toarcian vertebrates was favoured by a prolonged period of low bottom water oxygenation and accumulation rates. The environmental conditions that prevailed during the T-OAE were probably responsible for the extensive nature of Lagerstätte-type deposits with exceptional preservation of marine organisms. Whether the T-OAE had a biological impact on marine vertebrates requires a precise chemostratigraphic context of the fossil record spanning the Pliensbachian–Toarcian interval.

‘Supplementary material: [Geochemical dataset used in the present study including bulk sediment inorganic and organic carbon isotope composition ($\delta^{13}\text{C}$) and radiogenic strontium isotope ($^{87}\text{Sr}/^{86}\text{Sr}$) values of belemnites.] is available at XXX’.

69 The Early Jurassic Period was punctuated by severe environmental perturbations with
70 paroxysmal events coinciding with rapid biotic extinctions and turnover among
71 marine invertebrates across the transitions between the Pliensbachian-Toarcian stages
72 and the *tenuicostatum-serpentinum* ammonite zones (Little & Benton 1995; Harries &
73 Little 1999; Macchioni & Cecca 2002; Wignall *et al.* 2005; Suan *et al.* 2008; Caswell
74 *et al.* 2009; Suan *et al.* 2010; Ruebsam *et al.* 2019). The early-middle Toarcian also
75 witnessed the deposition of widespread laminated black shales resulting from a
76 prolonged episode of warmth and decreased bottom water oxygenation, which may
77 have favoured the preservation of abundant marine invertebrates and vertebrates (e.g.
78 Martill 1993). The interval of most intense environmental perturbation recorded in
79 strata spanning the uppermost part of the *tenuicostatum* ammonite zone to the top of
80 the *serpentinum* ammonite zone is known as the Toarcian Oceanic Anoxic Event (T-
81 OAE) (e.g. Jenkyns 1988; Baudin *et al.* 1990; Harries & Little 1999; Wignall *et al.*
82 2005; Caswell *et al.* 2009). Marine vertebrates were apparently little impacted by the
83 T-OAE (Vincent *et al.* 2013; Maxwell & Vincent 2016), although the records for the
84 time intervals pre- and post-dating these events are either scarce (Martin *et al.* 2012)
85 or poorly constrained stratigraphically.

86 Ichthyosaur remains are certainly the most ubiquitous marine vertebrates
87 found in Toarcian deposits of Europe with most iconic specimens reported from the
88 Posidonienschiefer Formation of the Holzmaden area in SW Germany. The most
89 spectacular exemplars include gravid females preserving soft tissues as well as
90 stomach contents (Böttcher 1989; 1990) and individuals preserving integuments
91 (Lindgren *et al.* 2018). Other remarkable finds include English specimens from
92 Ilminster in Somerset (Caine & Benton 2011; Williams *et al.* 2015) or the Alum Shale
93 Member in Yorkshire (Benton & Taylor 1984; McGowan & Motani 2003) but also
94 specimens preserving soft tissues from the Hettangian/Sinemurian of Dorset (Martill
95 1995).

96 Lagerstätte-type deposits during the Toarcian have been described mainly
97 from the Posidonienschiefer Formation in SW and NW Germany (Urlichs *et al.* 1994;
98 Hauff *et al.* 2017), Strawberry Bank and Whitby in England (Benton & Taylor 1984;
99 Benton & Spencer 1995; Williams *et al.* 2015), and, more recently, from the Ya Ha
100 Tinda locality in Alberta, Canada (Martindale *et al.* 2017). Three of these localities
101 (Posidonia Shale, Whitby and Ya Ha Tinda) are renowned for exceptionally-preserved
102 vertebrates occurring in organic-rich shales. Most of these shale-hosted specimens,

103 however, have been intensively impacted by burial compaction, which has exceeded
104 90% in such lithologies (Martill 1993), hence obscuring some important
105 morphological features, including details of skull bone contacts (e.g. Fraas 1913). On
106 the other hand, carbonate concretions with exceptional three-dimensional preservation
107 have been reported from Strawberry Bank as well as in a number of other Toarcian
108 localities (e.g. Normandy: Mazin 1988; northeastern Germany: Maisch & Ansorge
109 2004; Beaujolais: Vincent *et al.* 2013; Luxembourg: Vincent *et al.* 2019; see also
110 Table 1). Vertebrates preserved in carbonate concretions are potentially important
111 because they are comparatively less flattened than shale-hosted specimens. Given the
112 established presence of soft tissues in Toarcian marine vertebrates (e.g. Lindgren *et al.*
113 2018), carbonate concretions may also be promising for three-dimensional
114 reconstructions of soft tissues.

115 Regardless of their type of preservation, published Toarcian ichthyosaurs
116 generally lack a precise stratigraphic control, with the exception of most SW German
117 specimens that benefited from the early use of stratigraphic subdivisions of the
118 Posidonia Shale (Hauff 1921). The infra-stage stratigraphic data of previous
119 discoveries, if any, relied mostly on ammonite biostratigraphy (e.g. Benton & Taylor
120 1984; Godefroit 1994; Benton & Spencer 1995), in which resolution might be
121 strongly limited by both the abundance of age-diagnostic species and the use of
122 different bioevents in the various faunal provinces (Page 2003; McArthur *et al.* 2020).
123 Similarly, it is yet unclear whether vertebrate-hosting carbonate concretions are bound
124 to stratigraphically restricted horizons or occur randomly in Toarcian successions. In
125 this context, the massive accumulation of high-resolution isotope data fostered by the
126 growing interest for the T-OAE perturbations over the past decades could provide an
127 independent temporal framework for past and future vertebrate discoveries. Such a
128 multidisciplinary approach combining sedimentological, geochemical and
129 palaeontological data has been successfully used to replace important vertebrate
130 specimens in a detailed palaeoenvironmental and temporal framework and hence
131 better constrain conditions favouring their preservation (Suan *et al.* 2013; Vincent *et*
132 *al.* 2013; Vincent *et al.* 2020).

133 In this study, we briefly describe two new ichthyosaur specimens recovered
134 from our fieldwork in the LafargeHolcim Val d’Azergues quarry of Beaujolais, SE
135 France. We attempt to place the finds in a precise stratigraphic context using carbon
136 and strontium isotopes, allowing detailed age comparisons with coeval ichthyosaur-

137 yielding localities. We discuss the implications of our findings for the evolutionary
138 response of ichthyosaurs to Early Jurassic perturbations and the significance of
139 exceptional preservation, including that of soft tissues, for the prediction of similar
140 discoveries within Toarcian deposits.

141

142 **Institutional abbreviations**

143

144 **BRLSI**, Bath Royal Literary and Scientific Institution, Bath; **LGL-TPE**, Laboratoire
145 de Géologie de Lyon – Terre, Planètes, Environnements, Villeurbanne; **MHNL**,
146 Muséum d’Histoire Naturelle de Lyon/Musée des Confluences de Lyon, Lyon; **MHH**,
147 Museum Hauff, Holzmaden; **NHMUK**, Natural History Museum, London; **SMNS**,
148 Staatliches Museum für Naturkunde, Stuttgart.

149

150 **Lithology and biostratigraphy**

151

152 A synthetic account of the Lower Jurassic sedimentary succession available at the
153 LafargeHolcim Val d’Azergues quarry in Beaujolais (Rhône, SE France) is given
154 below. More detailed information is available from previous works (Vincent *et al.*
155 2013; Suan *et al.* 2013). The quarry exposes a marine sequence from the lower
156 Toarcian up to the upper Bajocian (Figs. 1, 2); the Toarcian – Aalenian
157 lithostratigraphy and ammonite biostratigraphy having been described by Elmi &
158 Rulleau (1991; 1993), and the complete succession was published by Rulleau (2006).
159 Here, we focus on the most recent excavations undertaken by our team during the
160 2009–2013 campaigns, revealing new observations and samplings of the lower
161 Toarcian interval, which was previously poorly known in the quarry (Rulleau 1997).
162 The basalmost lower Toarcian strata include a 2.5 m-thick succession of dolomitized
163 argillaceous yellowish limestone beds intercalated with yellow plastic clays. A
164 temporary trench realized in the lowermost levels in 2013 confirmed that these
165 lithologies are the weathered equivalent of grey, argillaceous limestone beds
166 intercalated with dark grey laminated marls with high total organic carbon contents
167 (up to 14% in weight; Charbonnier *et al.* 2020). This basal interval (‘Calcaires Jaunes
168 à Ammonitella’ in Elmi & Rulleau 1991) includes the *tenuicostatum* and *serpentinum*
169 ammonite zones (Elmi & Rulleau 1991; Suan *et al.* 2013). The *tenuicostatum* zone
170 was documented only in the basal bed, which yielded various dactylioceratid

171 ammonites of the *semicelatum* subzone (upper part of *tenuicostatum* Zone; e.g.
172 *Dactylioceras (Orthodactylites) semicelatum*, *D. (O.) crosbeyi*). The overlying 40 cm
173 of succession did not yield any ammonites. The presence of *Cleviceras elegans* in a
174 bed 50 cm above the base of the section and especially the co-occurrence of *C. elegans*
175 with *Harpoceras serpentinum* in nodular layers 70 and 120 cm above the base already
176 indicates the upper part of the *elegantulum* subzone (lower part of the *serpentinum*
177 Zone, equivalent of the *exaratum* subzone, see Page 2003). *Cleviceras elegans* was
178 collected also from beds 155 and 180 cm (bed with ichthyosaur specimen MHNL
179 20103062) above the base. However, this species can range up to the early *falciferum*
180 subzone (e.g. Bécaud, 2006) so these beds can thus either represent the upper
181 *elegantulum* subzone or the lower *falciferum* subzone. First age-diagnostic ammonites
182 of the *falciferum* subzone (upper part of the *serpentinum* Zone) represented by
183 *Harpoceras pseudoserpentinum* and *Hildaites subserpentinum* occur in the uppermost
184 bed, just below the dark marls. The yellowish limestone interval is capped by a
185 distinctive, 2-3 cm thick packstone-grainstone horizon mainly consisting of fish debris
186 and bivalves partly cemented by pyrite. The overlying 2.5 m-thick interval ('Marnes
187 inférieures' in Elmi & Rulleau 1991) of dark grey, finely laminated and
188 unfossiliferous calcareous marls, also often weathered into yellow plastic clays in the
189 quarry (Suan *et al.* 2013), yielded only few, poorly preserved ammonites and hence
190 lacks definitive ammonite zone assignment. Two fragmentary specimens of
191 *Harpoceras falciferum* were collected about 90 cm above the base of the marly
192 interval. Although this species is typical of the upper part of the *falciferum* subzone,
193 its upper stratigraphic range limit is located in the *sublevisoni* subzone of the early
194 *bifrons* Zone (e.g. Elmi *et al.* 1997). The calcareous nannofossil association and
195 ⁸⁷Sr/⁸⁶Sr values (see below) indicate that this level with *H. falciferum* fragments
196 probably belongs to the *sublevisoni* subzone. This marly interval is overlain by a 2.4
197 m-thick succession of intensively bioturbated marl containing iron ooids and abundant
198 invertebrates, including age-diagnostic ammonites of the *bifrons* (middle Toarcian)
199 and *variabilis* (upper Toarcian) ammonite zones and various vertebrate remains (e.g.
200 Vincent *et al.* 2013). The base of this interval yielded the articulated skeleton of the
201 ichthyosaur *Temnodontosaurus azerguensis* (Martin *et al.* 2012). Apart from the
202 almost unfossiliferous interval of dark grey marls between 2.5 and 5.2 m, the
203 investigated succession is relatively well-constrained biostratigraphically owing to its
204 ammonite richness. Nannofossil data may offer additional temporal constraints. The

205 first occurrence of *Watznaueria colacicchii*, recorded at 3.3 m in the ammonite-barren
206 interval in the LafargeHolcim Val d’Azergues Quarry (Suan *et al.* 2013), has been
207 recently shown to coincide with the base of the *bifrons* Zone in Portugal (Ferreira *et*
208 *al.* 2019; base of nannofossil NTJ7b Zone). Pending future ammonite discoveries and
209 further chemostratigraphic assessment (see below), the base of the *bifrons* Zone
210 should hence certainly occur below that suggested by sparse ammonite record of
211 *Harpoceras faciferum*, i.e., toward the lower half of the ammonite-barren interval.

212 The Posidonienschiefer Formation (Posidonia Shale; Lias epsilon) of
213 Southwestern Germany has been divided into lower, middle, and upper components
214 indicated by roman numerals (I-III), with beds within these larger subdivisions
215 indicated using subscript. When comparing the biostratigraphy to the divisions
216 recorded in the Southwest German Basin, we use the bed-level nomenclature and
217 ammonite zone correlations detailed by Riegraf *et al.* (1984).

218

219 **Material and methods**

220

221 **Fieldwork and specimen preparation.** We report on two ichthyosaur specimens
222 discovered during our palaeontological excavations in 2010 and 2012 at
223 LafargeHolcim Val d’Azergues cement Quarry near Charnay in the Beaujolais hills
224 (Rhône, France). Both specimens are repositated at the Musée des Confluences, Lyon,
225 France. The first specimen (MHNL 20103062) was discovered in July 2010 in a thin
226 limestone bed at 1.8 m during manual excavation of the interval between 1.6 and 2.5
227 m (*serpentinum* Zone). The second specimen was discovered in the material
228 excavated mechanically by a bulldozer from the first 2.5 m of the measured interval in
229 July 2012 (*serpentinum* ammonite Zone). MHNL 20103062 was prepared during
230 2013 by one of us (AC) at Institut des Sciences de l’Evolution, Université de
231 Montpellier, alternating mechanical preparation and weak acetic acid baths in order to
232 soften the sediment without damaging the bone surface. The second specimen
233 (MHNL 20103364), preserved in a large carbonate concretion with possible soft
234 tissues, awaits preparation and is temporarily deposited at LGL-TPE for ongoing
235 study before its permanent curation at Musée des Confluences (MHNL). These recent
236 findings extend the relatively rich record of ichthyosaurs of this site (Vincent *et al.*
237 2013), initiated in 1984 with the discovery of a subcomplete specimen, which was

238 recently described and attributed to *Temnodontosaurus azerguensis* (Martin *et al.*
239 2012).

240

241 **Chemostratigraphy.** In order to place the recently discovered specimens from the
242 LafargeHolcim Val d’Azergues quarry into a stratigraphic context, we analyzed the
243 bulk sediment inorganic and organic carbon isotope composition as well as the
244 strontium isotope composition of belemnites, all collected from the section that
245 yielded the three ichthyosaur specimens. We also analyzed the inorganic carbon
246 isotope composition of a sample collected from the carbonate concretion containing
247 the specimen discovered in 2012 to narrow down its likely provenance. The
248 stratigraphic log of the study site, modified from Suan *et al.* (2013) and updated with
249 these new geochemical data (Supplementary Data), is shown in Figure 2.

250 A total of 43 samples (including the sample collected from the ichthyosaur-
251 hosting carbonate concretion), consisting of both weathered and non-weathered
252 sediment, were analyzed for their bulk carbonate carbon isotope ($\delta^{13}\text{C}_{\text{carb}}$) composition
253 using an auto sampler MultiPrep™ system coupled to a dual-inlet GV IsoPrime™
254 isotope ratio mass spectrometer (IRMS). Each sample was powdered in an agate
255 mortar and, depending on calcium carbonate contents, an aliquot of 200-2000 μg of
256 the obtained powder was reacted with anhydrous, oversaturated phosphoric acid at
257 90°C for 20 min. Each analytical run contained international (NIST NBS19) and in-
258 house standards (Carrara Marble) to monitor analytical precision and accuracy.

259 A total of 22 samples were analyzed for their organic carbon isotope
260 composition ($\delta^{13}\text{C}_{\text{TOC}}$). To avoid potentially strong weathering biases on the measured
261 $\delta^{13}\text{C}_{\text{TOC}}$ values (Suan *et al.* 2013), only samples that appeared non-weathered under
262 visual examination (dark colour, absence of orange-brownish oxidation stains) were
263 selected. Each sample was powdered in an agate mortar and decarbonated using 1N
264 hydrochloric acid at ambient temperature overnight. Each sample was sequentially
265 rinsed four times with deionized water, with 40 minutes between rinses to allow the
266 sediment to settle, and oven-dried at 40°C. Between 0.5 and 1 mg of decarbonated
267 powder was weighted into tin capsules and placed in a Pyrocube® elemental analyzer
268 connected to an Elementar IsoPrime® isotope-ratio mass spectrometer in continuous
269 flow. Each analytical run contained four sets of international (IAEA-CH-7) and in-
270 house standards (Caseine) to monitor analytical precision and accuracy. All carbon
271 isotope results are reported relative to the ‘Vienna Pee Dee belemnite’ (VPDB). Based

272 upon replicated analysis of standards, the precision of our measurements was better
273 than $\pm 0.1\text{‰}$ for $\delta^{13}\text{C}_{\text{TOC}}$ values and $\pm 0.05\text{‰}$ for $\delta^{13}\text{C}_{\text{carb}}$ values.

274 We sampled five belemnites for radiogenic strontium analysis ($^{87}\text{Sr}/^{86}\text{Sr}$) from
275 different levels in the lower and middle Toarcian interval. For each sample, the
276 rostrum was broken into millimeter-size fragments to select the best-preserved portion
277 of the samples. Fragments showing a strong radial fabric were subsequently picked
278 (avoiding the apical line and external-most areas) under a binocular microscope and
279 powdered in an agate mortar. About 2 mg of belemnite powder was dissolved in
280 concentrated nitric acid and evaporated to dryness. All samples were retaken in 2M
281 HNO_3 and purified through a strontium-specific resin (Sr-Spec Eichrom®). The
282 obtained solution was analyzed for $^{87}\text{Sr}/^{86}\text{Sr}$ ratios at LGLTPE on a Neptune Plus
283 multicollector ICP-MS (Thermo Scientific) during a single session in December 2014.
284 Reference material (SRM-987) of known $^{87}\text{Sr}/^{86}\text{Sr}$ composition was repeatedly
285 measured in the same analytical session. The standard SRM-987 gave an average
286 value of 0.7100912 ± 0.00000356 (1SD, $n = 5$), which is within 0.0001568 of the
287 value 0.710248 (McArthur *et al.* 2000). Belemnite values were adjusted accordingly
288 and are listed in the Supplementary Data.

289

290 **Results**

291

292 **Carbon and strontium isotope composition.** The $\delta^{13}\text{C}_{\text{carb}}$ profile, although somewhat
293 scattered, reveals a marked $>3\text{‰}$ decrease across the *tenuicostatum-serpentinum* zonal
294 transition and a $>4\text{‰}$ increase between 0.3 and 1 m. The $\delta^{13}\text{C}_{\text{TOC}}$ values of non-
295 weathered samples show minimal values (down to -32‰) at the very base of the
296 *serpentinum* ammonite Zone, and a marked 2.4‰ increase between 0.3 and 0.6 m.
297 These new records, when combined with previously published data from the same site
298 (Suan *et al.* 2013; Fig. 2), show that the characteristic T-OAE negative carbon isotope
299 excursion of the *serpentinum* Zone is restricted to the first 0.70 m of the studied
300 section. In particular, the extremely low $\delta^{13}\text{C}_{\text{TOC}}$ values recorded between 0.3 and 0.5
301 m are comparable to those recorded in most other contemporary sections in the base
302 of the T-OAE interval (-30 to -34‰) (Suan *et al.* 2016; 2018). The sedimentary
303 matrix of the large carbonate concretion found during the excavation of the trench in
304 the basal 2.5 m interval yielded a $\delta^{13}\text{C}_{\text{carb}}$ value of -3.88‰ . Comparatively low values
305 are only recorded in the interval comprised between 0.2 and 0.5 m at the very base of

306 the *serpentinum* Zone in our composite $\delta^{13}\text{C}_{\text{carb}}$ profile, constraining its likely
307 provenance (Fig. 2).

308 The obtained $^{87}\text{Sr}/^{86}\text{Sr}$ values for the analyzed Toarcian belemnites range
309 between 0.70710095 and 0.707227, consistent with the range of values obtained for
310 this interval in previous studies (McArthur *et al.* 2000; Bailey *et al.* 2003). Our
311 $^{87}\text{Sr}/^{86}\text{Sr}$ profile records a marked shift toward more radiogenic values at the base of
312 the measured section, the amplitude of which is compatible with that observed across
313 the *tenuicostatum-serpentinum* transition in SW Germany and NE England (McArthur
314 *et al.* 2000; Bailey *et al.* 2003). The belemnite specimen sampled in the argillaceous
315 marl located 2 cm below the ichthyosaur specimen MHNL 20103062 yielded a
316 $^{87}\text{Sr}/^{86}\text{Sr}$ value of 0.707194. Comparably high values are only found in the uppermost
317 part of the *serpentinum* Zone in both German (Fig. 2b) and English sites (McArthur *et*
318 *al.* 2000; Bailey *et al.* 2003), where the boundary between the *serpentinum-bifrons*
319 zones is biostratigraphically better constrained than in the Val d’Azergues Quarry. In
320 Yorkshire, such values occur immediately below the base of the Alum Shale Member
321 (McArthur *et al.* 2000), which has yielded historically important marine vertebrate
322 specimens (Benton & Taylor 1984). In the Val d’Azergues Quarry, the belemnite
323 collected in the same bed as the *Temnodontosaurus azerguensis* specimen (Martin *et*
324 *al.* 2012), *i.e.* in the *bifrons* ammonite subzone (*bifrons* zone), gave a $^{87}\text{Sr}/^{86}\text{Sr}$ value of
325 0.7072229. In Yorkshire, comparable values occur above the base of the *crassum*
326 subzone, which correspond to the topmost part of the Alum Shale Member (*bifrons*
327 zone; McArthur *et al.* 2000). The $^{87}\text{Sr}/^{86}\text{Sr}$ value of 0.707227 measured in the
328 uppermost sample from the *variabilis* ammonite zone is consistent with values
329 measured in the middle of the *variabilis* zone in Yorkshire. Within the temporal
330 resolution allowed by the Toarcian strontium isotope stratigraphy (< 200 ka,
331 McArthur *et al.* 2020), these $^{87}\text{Sr}/^{86}\text{Sr}$ data support the synchronicity of Subboreal and
332 Submediterranean ammonite Subzones that have been respectively used in Yorkshire
333 and SE France (Elmi *et al.* 1997; Page 2003). In summary, the obtained carbon and
334 strontium isotope data enhance correlations with the classical localities of SW
335 Germany (Fig. 2) and Yorkshire, hence enabling detailed relative dating of the various
336 Toarcian ichthyosaur finds and their relationships with the coeval environmental
337 perturbations (see below).

338

339 **Description of Ichthyosaur MHNL 20103062.** Specimen MHNL 20103062
340 preserves most of the skull and the anterior part of the mandible. The rostrum is
341 complete with an antorbital length of 43 cm and a prenarial length of 35 cm. Despite
342 being partly disarticulated, it preserves fine anatomical details including bones
343 preserved in volume and sutures in the peri-orbital region. The left lateral side of the
344 specimen is exposed. The skull lacks the posteriormost part of the braincase and is
345 split along the sagittal axis. The right elements of the skull are disarticulated and have
346 been displaced dorsally; the top of the right portion of the skull table faces laterally.
347 Because the postorbital region in ichthyosaurs is short, a rough total skull length can
348 be estimated and would not have surpassed 60 cm.

349 The large circular orbit measures 10 cm in diameter. It is bordered ventrally by
350 the jugal, anteroventrally by the lacrimal, anteriorly and anterodorsally by the
351 prefrontal and posteriorly by the postorbital. The left sclerotic ring is 9 cm in diameter
352 and its aperture diameter is 3.6 cm. The aperture diameter to the orbital diameter
353 versus skull length ratio of Fernández *et al.* (2005) compares well (0.23) with the
354 values of other adult specimens of the genus *Stenopterygius*. The sclerotic ring is
355 complete and articulated with 14 individual sclerotic plates. The plates overlap each
356 other but there is no clockwise or anti-clockwise trend.

357 The premaxilla contributes to most of the rostrum. The lateral surface bears a
358 set of small foramina that are placed at the level of a long groove that extends
359 posteriorly on the lateral surface of the bone. There are no individualized tooth
360 sockets, the implantation is aulacodont. There are at least 30 alveolar positions
361 deduced by incipient concavities on the bone. The subnarial process of the premaxilla
362 projects below the external nares but does not contact the anteriormost tip of the jugal,
363 being separated from the ventral margin of the external nares by the underlying
364 maxilla. The supranarial process of the premaxilla is short.

365 The maxilla separates the premaxilla and lacrimal from any contact. The
366 maxilla contributes to the anterior ventral half of the external nares. The maxilla
367 supports the premaxillary lamina anteriorly, and posterodorsally possesses a long
368 sutural contact with the jugal. Dorsally, the maxilla contacts the lacrimal, separating
369 the jugal from the external nares. In the anteriormost corner of the external nares, the
370 maxilla contacts the descending process of the nasal. The maxillary tooth row stops
371 below the orbit in the anteriormost orbital area.

372 The nasal contributes dorsally to the external naris for its entire length. Here,
373 an overhanging crest projects laterally above the external naris (Fig. 3).
374 Anteroventrally, the nasal descends along the anterior edge of the external nares,
375 excluding the premaxilla from the external nares and suturing ventrally onto the
376 maxilla. Posteriorly, in lateral view the nasal contacts the lacrimal and prefrontal.
377 Because the skull is split in half, it is difficult to ascertain the presence of an internasal
378 depression on the dorsal surface of the skull.

379 The lacrimal contributes to the posterior and posteroventral margins of the
380 external nares. The anteriormost tip of the lacrimal consists of a delicate notch
381 projecting medially to the maxilla, along the ventral border of the external nares. The
382 lacrimal contacts the nasal dorsally, along the posterior margin of the external nares,
383 excluding the prefrontal from the narial opening. This suture stops just below the
384 dorsal edge of the external nares. The circumorbital area of the lacrimal is heavily
385 vascularized. The ventral margin of the lacrimal mostly contacts the jugal, with the
386 exception of its anterior part, which contacts the maxilla. The lacrimal has an oblique
387 and indented suture with the prefrontal on the orbital margin.

388 The prefrontal forms the anterodorsal margin of the orbit. The bone is
389 anteroposteriorly thin, preventing the nasal from reaching the orbital margin. As
390 observed in dorsal view (Fig. 3), the prefrontal is constricted between the nasal and
391 postfrontal and contacts the frontal and parietal near its medial margin.

392 The jugal anterior tip projects beyond the anterior margin of the orbits as a
393 thin lamina. Here, it overlaps the maxilla ventrally and the lacrimal dorsally. The
394 jugal forms the majority of the ventral border of the orbit; the anteroventral border of
395 the orbit is made by a thin lamina of the lacrimal overlapping the jugal. The posterior
396 portion of the jugal sends a short dorsal extension along the orbital edge as a
397 mediolaterally flat ascending lamina.

398 Bones of the skull table include a complete right frontal and fragmentary left
399 frontal, a right postfrontal, fragmentary left postorbital and right parietal. The anterior
400 margin of the interfrontal foramen wedges between the posterior ends of the nasals.
401 There is no extension of the interfrontal fossa on the nasal. This fossa is exclusively
402 restricted to the frontals.

403 Both frontals are sutured in their posterior region, but for most of their length
404 they never contact. Their dorsal surface is steeply inclined toward the midline where
405 they accommodate the elongate interfrontal foramen. The frontals contact the nasal at

406 the anterior edge of the interfrontal foramen. Laterally, the frontal contacts the
407 prefrontal and posteriorly, it contacts the parietal. Posteriorly, the frontal forms the
408 anterolateral margin of the pineal foramen as in most post-Triassic ichthyosaurs
409 (Maisch & Matzke 2000). The pineal foramen preserves only its anterior portion,
410 missing the posteriormost margin. It opens dorsally with an anteriorly rounded outline
411 (about 0.7 cm in diameter) on the sagittal axis at the frontoparietal suture.

412 The postfrontal forms the anterior margin of the supratemporal fenestra where
413 it consists of a thickened rim. Anterior to this rim, the rest of the dorsal surface of the
414 postfrontal is concave. Its lateral area is triangular and overhangs the orbits laterally.
415 The postfrontal contacts the prefrontal anteriorly along a sinuous suture.
416 Posteromedially, it contacts the parietal.

417 The postorbital consists of a wide lamina that makes the posterior margin of
418 the orbit and contacts the posterior ascending process of the jugal. On the
419 posteriormost margin of the postorbital, a long lamina is observed and might
420 correspond to a fragment of the squamosal or quadratojugal.

421 A small fragment of the right parietal is visible (Fig. 3). In its anterior portion,
422 the parietal makes the lateral margin of the pineal foramen, and contacts the frontal
423 anteriorly and also the postfrontal laterally. Although fragmented, the parietal appears
424 to participate in the medial margin of the supratemporal fenestra.

425 The mandible has partially been recovered and includes the anteriormost rami
426 of both dentaries. The dentary is a straight bone with a flat and long dentary
427 symphysis. The tooth row is confluent for the entire preserved length.

428 A single tooth is still attached to the premaxilla but all other teeth were
429 recovered detached from the premaxilla, maxilla and dentary in the surrounding
430 sediment, the block revealing 10 detached teeth (Fig. 3). The crowns are narrow,
431 pointed, slender, recurved and rounded in cross section (Fig. 4). The enamel surface
432 bears no carinae and is unornamented. The root has the characteristic plicidentine
433 morphology with deep furrows on the external surface giving the typical cauliflower
434 outline in cross section. Roots are only slightly more than half the total length of the
435 tooth.

436

437 **Ichthyosaur from the carbonate concretion.** The second specimen (MHNL
438 20103364, Fig. 5) was discovered during the summer of 2012 when a trench on the
439 floor of the LafargeHolcim Val d'Azergues quarry was excavated thanks to heavy-

440 duty vehicles, allowing us to attain the lowest stratigraphic horizons available in the
441 quarry (Figs. 1a, 5a). As presented above, this specimen, together with other
442 carbonate concretions, originates from the base of the *serpentinum* ammonite zone.
443 The ichthyosaur specimen is contained in a large carbonate concretion measuring
444 about 50 cm in diameter. Breaks on its surface reveal an articulated skeleton with the
445 extremity of the rostrum at one end (Fig. 5c), and opposite, a paddle (Fig. 5b) and a
446 section in the thorax with articulated vertebral centra and ribs (Fig. 5d). The specimen
447 is curled around one side of the carbonate concretion and sectioned at the level of the
448 thorax, missing the tail. Nonetheless, the anterior part of the rostrum is sectioned and
449 shows several tooth roots; opposite the rostrum on the carbonate concretion, the
450 forefin is partly visible and displays at least four phalanges (Fig. 5b). The phalanges
451 are not in contact and possess rounded edges. Those characters are compatible with
452 the morphology of distal phalanges of stenopterygiids. The total body length of the
453 specimen cannot be precisely measured but may not have surpassed one meter.
454 Reddish to purple hues are observed within the rib cage and most likely represent
455 remnants of soft tissues (Figs. 5d, e, f), to be investigated in future work, for example
456 through X ray Computed Tomography in order to avoid destroying soft tissue during
457 preparation.

458

459 **Discussion**

460

461 **Affinities of the new finds.** Currently recognized Toarcian ichthyosaur genera
462 include *Eurhinosaurus*, *Hauffiopteryx*, *Temnodontosaurus*, *Stenopterygius* and
463 *Suevoleviathan* (e.g. McGowan 1979; Godefroit 1994; McGowan & Motani 2003;
464 Fischer *et al.* 2012; Caine & Benton 2012; Martin *et al.* 2012; Maxwell 2012; Moon
465 2017; Maxwell & Cortés 2020).

466 MHNL 20103062 does not preserve any postcranial elements, which are
467 prominent in ichthyosaur diagnoses (Maxwell 2012). Ichthyosaurs from the Posidonia
468 Shale are often preserved as flattened complete skeletons but details of their skull
469 anatomy may be obscured by compression. As a consequence, diagnostic characters
470 for species have been established on skull proportions and postcranial anatomy
471 (McGowan 1979) with species delineation relying mostly on postcranial proportions
472 (Maxwell 2012). Nevertheless, a number of cranial features can be compared with
473 other Jurassic forms and help constrain the affinities of MHNL 20103062.

474 MHNL 20103062 can be differentiated from the large predatory species of the
475 genus *Temnodontosaurus* in which the maxilla does not contribute into the ventral
476 margin of the external narial opening, in contrast to that of MHNL 20103062 (Fig. 4).
477 In toothed *Temnodontosaurus* species, the maxilla is excluded from the narial opening
478 by the subnarial process of the premaxilla contacting the lacrimal and jugal
479 (McGowan 1994; Maisch 1998a). In MHNL 20103062, the nasal does not contact the
480 parietal posteriorly, contrary to species of the genus *Temnodontosaurus* (Maxwell *et*
481 *al.* 2012; Ji *et al.* 2015). MHNL 20103062 can be differentiated from *T. azerguensis*
482 in possessing teeth (Martin *et al.* 2012).

483 *Eurhinosaurus longirostris* is extremely derived among Toarcian ichthyosaurs,
484 with its particularly elongate rostrum that parallels the morphology of extant billfishes
485 and swordfishes (e.g. McGowan 1979). Although the rostrum is elongate in MHNL
486 20103062, it is comparatively much shorter than that of *E. longirostris*.

487 MHNL 20103062 can be differentiated from *Hauffiopteryx* based on the
488 absence of participation of the prefrontal in the external narial opening (see Maxwell
489 & Cortés, 2020). In addition, the pineal foramen is positioned between the
490 supratemporal fenestrae in MHNL 20103062; it opens anterior to the supratemporal
491 fenestrae in *Hauffiopteryx*. In *Hauffiopteryx*, the anterior margin of the supratemporal
492 fenestra consists of the parietal (not of the postfrontal as in MHNL 20103062); the
493 prefrontal is constricted between its lateral and medial parts in MHNL 20103062, but
494 of uniform width in *Hauffiopteryx*; the comparatively shorter rostrum of
495 *Hauffiopteryx* and its differential tooth size between fore and aft dentition, also differ
496 from MHNL 20103062 (Maisch 2008; Caine & Benton 2011; Marek *et al.* 2015;
497 Maxwell & Cortés 2020).

498 *Suevoleviathan* differs from MHNL 20103062 in that the lacrimal and
499 subnarial process of the prefrontal exclude the maxilla from the ventral edge of the
500 narial opening in lateral view, the descending process of the prefrontal is much more
501 weakly developed, the medial process of the prefrontal contacting the parietal and
502 frontal is absent in dorsal view, and the frontal contributes only to the anterior edge of
503 the parietal foramen rather than forming the anterior and lateral edges (Maisch 1998b;
504 2001).

505 Other Early Jurassic ichthyosaurs such as the genera *Ichthyosaurus* and
506 *Protoichthyosaurus* are distinct from MHNL 20103062, in that the tooth enamel in
507 these genera bears a strongly ridged ornamentation, unlike in MHNL 20103062.

508 These genera also have a medial process of the prefrontal contacting both the parietal
509 and frontal (see Lomax *et al.* 2020). This latter character is shared with the genus
510 *Leptonectes* (Fig. 2 in Maisch & Matzke 2003). In MHNL 20103062, the anterior
511 margin of the supratemporal fenestra consists of the postfrontal, without a large
512 contribution from the parietal (unlike in *Leptonectes* and *Wahlisaurus*: Maisch &
513 Matzke 2003; Lomax *et al.* 2018). In *Leptonectes tenuirostris*, the subnarial and
514 supranarial processes of the premaxilla are subequal in length (McGowan & Motani
515 2003: fig. 69).

516 MHNL 20103062 can be identified as a member of the genus *Stenopterygius*
517 on the basis of the following skull characters: In MHNL 20103062, the supranarial
518 process of the premaxilla is substantially shorter than the subnarial process (Figs. 3,
519 4), a condition shared with the genus *Stenopterygius*. Since the work of Maxwell
520 (2012), several species of *Stenopterygius* have been synonymized and we follow it,
521 recognizing the genus *Stenopterygius* as containing four European species, *S.*
522 *quadriscissus*, *S. uniter* *S. triscissus*, and *S. aaleniensis*, plus a South American one *S.*
523 *cayi* (Fernández 1994). MHNL 20103062 differs from some specimens of *S. triscissus*
524 (see specimen BRLSI M1409 studied by Caine & Benton 2011) in the lack of contact
525 between premaxilla and lacrimal; however note that this feature varies
526 intraspecifically in *Stenopterygius* (e.g., *S. triscissus*: compare Caine & Benton 2011:
527 text-fig.3; Godefroit 1994: fig. 19). Also, the absence of contact between nasal and
528 parietal contrasts with the state reported for some specimens of *S. triscissus* (Caine &
529 Benton 2011), but not for others (Motani 2005). The contact reported by Caine &
530 Benton (2011) is very thin in this juvenile specimen from Strawberry Bank; this
531 character is likely to be intraspecifically variable. The pineal foramen opens in
532 different ways among members of the genus *Stenopterygius*: (1) the pineal foramen is
533 included between the supratemporal fenestrae; or (2) the pineal foramen opens just
534 anterior to the supratemporal fenestrae. MHNL 20103062, many Curcy specimens
535 (Mazin 1988 plate I; *S. triscissus*: NHMUK OR 33157(Caine & Benton 2011: text-
536 fig. S3), Eudes-Deslongchamps 1877)) and an Ilminster *S. triscissus* specimen
537 (BRLSI M1409) (Caine & Benton 2011) all share condition (1). Some Holzmaden
538 *Stenopterygius* specimens in which the skull table is visible show condition (2) such
539 as in some specimens of *S. quadriscissus* (MHH 1981/33 or SMNS 55933) or *S.*
540 *triscissus* (SMNS 14846). Differences are also noted with *S. aaleniensis*, which
541 possesses an embayment in the posterior dorsal corner of the external nares (Maxwell

542 *et al.* 2012), absent in MHNL 20103062. MHNL 20103062 differs from the South
543 American *S. cavi*, which lacks teeth (Fernández 1994). Tooth reduction is variably
544 present in all three Toarcian species of *Stenopterygius*, with some adult specimens
545 possessing unreduced dentition while others are functionally edentulous (Maxwell
546 2012; Dick & Maxwell 2015; Dick *et al.* 2016).

547 The specimen from the large carbonate concretion is unprepared and cannot be
548 precisely identified beyond a tentative referral to Stenopterygiidae indet. based on the
549 characters visible on the rostrum and forefin.

550 In conclusion, MHNL 20103062 is referable to the genus *Stenopterygius*, and
551 because it is represented only by a skull, we refrain from further specific attribution
552 and refer it to *Stenopterygius* sp.. However, the prenatal length of 35 cm is outside
553 the range of *S. quadriscissus* (see Maxwell 2012), making referral to the latter species
554 unlikely. The carbonate concretion specimen is a probable stenopterygiid, but this will
555 have to be confirmed with further preparation.

556

557 **Ichthyosaur preservation during the T-OAE.** Preservation of marine vertebrates in
558 Lower Jurassic carbonate concretions (as compiled in Table 1) is known at least since
559 the discovery of the Strawberry Bank Lagerstätte (Lower Toarcian of Ilminster,
560 Somerset) by Charles Moore in the late 1840s (Williams *et al.* 2015). This locality has
561 yielded carbonate concretions containing finely preserved ichthyosaur skeletons that
562 were studied much later (McGowan 1979) and only recently referred to
563 *Stenopterygius triscissus* and *Hauffiopteryx typicus* (Caine & Benton 2011; Marek *et*
564 *al.* 2015). Elsewhere, ichthyosaur skulls preserved in similar carbonate concretions
565 have subsequently been reported from the Toarcian of Luxembourg with
566 *Stenopterygius* (Godefroit 1994) and France including *Temnodontosaurus burgundiae*
567 from Sainte-Colombe in Burgundy (Gaudry 1892) and specimens from Curcy-sur-
568 Orne in Normandy (Dechaseaux 1954) including an acid prepared carbonate
569 concretion containing a skull connected to postcranial elements of *Stenopterygius*
570 (Mazin 1988). A 9-meter long complete individual of *Temnodontosaurus* (SMNS
571 50000) mostly preserved within a giant carbonate concretion was discovered from
572 horizon epsilon II₆ between Zell unter Aichelberg and Ohmden (Böttcher 1989).
573 Large carbonate concretions within the upper part of horizon epsilon II₄ yielded at
574 least two specimens on display at the Dotternhausen Museum including
575 *Stenopterygius* and *Hauffiopteryx* (Jäger 2005; Maxwell & Cortés 2020). A specimen

576 of *Stenopterygius quadriscissus* (SMNS 4789) is not technically speaking within a
577 concretion but hosts pyrite in the thoracic area and also originates from epsilon II₅ and
578 was selected for histological analysis (Anderson *et al.* 2018). Additional skulls and
579 fragmentary ichthyosaurian postcranial remains from the Holzmaden region preserved
580 in concretions are also present in regional collections. The difficulty in preparing
581 specimens from hard concretions partially accounts for the rarity of described
582 specimens in the literature originating from nodular beds and also the heavily lithified
583 epsilon II₅ level. In addition, *Stenopterygius* specimens in concretions do not typically
584 preserve enough of the skeleton to allow referral to species, which requires relatively
585 complete skeletons at present (but see *S. aalenensis* in Maxwell *et al.* 2012). This
586 results in a perceived gap in the fossil record of species in the genus (e.g. Fig. 2 in
587 Maxwell 2012).

588 Williams *et al.* (2015) described the Strawberry Bank carbonate concretions as
589 biomicritic mudstones to packstones containing invertebrate bioclasts. Carbonate
590 concretions are often weathered to a yellowish colour, as is the surrounding sediment,
591 although originally, the unaltered deposits were blue-grey (Moore 1866) with high
592 organic content (Suan *et al.* 2013; Charbonnier *et al.* 2020). Under anoxic conditions,
593 the presence of organic matter in mudstone boosts the formation of concretions early
594 during diagenesis; microbial activity produces methane and carbon dioxide that
595 provide the basis for carbonate precipitation and nucleation (Raiswell 1988; Raiswell
596 & Fisher 2000; Marshall & Pirrie 2013). Within most Toarcian levels with organic-
597 rich shales, specimens have undergone compaction and even if soft tissues have been
598 positively identified, their flatness hides many morphological features. The interesting
599 prospect is that levels with concretions are known within these organic-rich shales and
600 due to their early diagenetic implementation, hold the potential of preserving
601 vertebrate specimens, including soft tissues, in volume.

602 Several ichthyosaur specimens from the Toarcian of SW Germany and, to a
603 lesser extent, of England are known to preserve soft tissue including skin and muscle
604 fibers preserved as phosphatized or carbonized films (Fraas 1888; Martill 1993;
605 Lingham-Soliar 1999). Ichthyosaurs with extensive soft tissue remains have been
606 reported from a number of beds within the Posidonienschiefer Formation,
607 predominantly in the laminated black shales extending from the upper part of the
608 *tenuicostatum* Zone into the *serpentinum* Zone, specifically from epsilon II₁,
609 (*semicelatum* subzone) to epsilon II₈ (*elegans* subzone), with most soft-tissue

610 specimens originating from epsilon II₃–II₄ (Hauff 1921; Hofmann 1958; Keller 1992;
611 Martill 1993). A slightly broader stratigraphic range for soft tissue preservation was
612 presented by Heller (1966), including specimens from epsilon II₉ and epsilon II₁₀
613 (*falciferum* subzone), suggesting that soft-tissue preservation, as concerns Toarcian
614 deposits, may not be limited to laminated black shales and the epsilon II₅ laminated
615 limestone. However, the best-preserved examples are from the laminated sediments.
616 Recent studies using geochemical, ultrastructural and molecular tools have helped
617 characterize the preservation of different soft tissue types from deposits of the
618 Posidonienschiefer Formation in SW Germany. As such, a carbonate concretion from
619 Dotternhausen containing an individual of *Stenopterygius* preserves structures
620 resembling collagen as well as red and white blood cells (Plet *et al.* 2017); another
621 *Stenopterygius* specimen preserved on a mudstone slab from the early Toarcian from
622 Kromer Shale Quarry near Ohmden shows integument likely preserving blubber,
623 melanophores as well as various lipids and proteins (Lindgren *et al.* 2018).

624 Our geochemical data ($\delta^{13}\text{C}$ and $^{87}\text{Sr}/^{86}\text{Sr}$) help to constrain the stratigraphic
625 origin of the newly reported specimens. These data show that MHNL 20103062
626 comes from the middle part of the *serpentinum* ammonite zone, i.e. after the T-OAE
627 carbon isotope excursion (Fig. 2). This specimen is partly disarticulated and not
628 preserved in a carbonate concretion but at the base of a normally graded argillaceous
629 limestone bed likely corresponding to a tempestite (Suan *et al.* 2013). The preparation
630 of this specimen revealed a discontinuous, millimeter-sized crust of goethite covering
631 the stratigraphically lowermost surface of the bones as well as the sediment located
632 between the left and right premaxillae. This goethite crust, still partly visible as rust-
633 coloured stains on and in between some bones in the prepared specimen (Fig. 3),
634 likely corresponds to a completely oxidized pyrite crust. Comparable pyrite coatings
635 described in some other Konservat Lagerstätten have been interpreted as a
636 consequence of microbial degradation of organic-rich tissues (Muscente *et al.* 2017).
637 The specimen therefore certainly did preserve soft tissues replaced by pyrite
638 (subsequently weathered into goethite).

639 The geochemical data indicate that the oldest ichthyosaur specimen reported
640 here and preserved in connection within a carbonate concretion was most likely
641 derived from the very base of the *serpentinum* ammonite zone (Fig. 2) within the
642 interval recording the T-OAE negative carbon isotope excursion. We highly suspect
643 the preservation of soft tissue in the carbonate concretion specimen, as evidenced

644 from oxidized features contained exclusively within the rib cage (Fig. 7d–f). In
645 addition, chemo- and biostratigraphic constraints enable detailed temporal correlations
646 between our finds from Beaujolais and coeval finds from SW Germany (Fig. 2).

647 At the scale of a given locality, there seems to be no specific horizon yielding
648 complete specimens with soft tissues and a close examination of other similar (in age
649 and sedimentological characteristics) paleontological localities may confirm this
650 hypothesis. However, the occurrence of carbonate concretions containing marine
651 vertebrates seems to correspond to the T-OAE interval, and depending on the
652 thickness of the deposit as observed across European localities, several horizons with
653 carbonate concretions may be recovered during this particular environmental
654 perturbation. For example, the succession at LafargeHolcim Val d’Azergues quarry is
655 condensed and such carbonate concretions were predicted to occur in the lower part of
656 the *serpentinum* Zone, where the negative carbon isotope excursion is recorded. The
657 original collector at Strawberry Bank only described one such horizon, and though the
658 precise location of that quarry is enigmatic, this observation was corroborated by an
659 excavation in close proximity in 2019 led by MW. As for the historical locality of La
660 Caine, prospecting for carbonate concretions in the field will have to be undertaken.
661 In Belgium and Luxembourg, several marine reptile specimens have been reported
662 between the *tenuicostatum* and *serpentinum* ammonite zones (Godefroit 1994;
663 Vincent *et al.* 2019), but a more detailed placement against carbon isotope
664 stratigraphy established for this area (Ruebsam *et al.* 2016; Hermoso *et al.* 2014)
665 would deserve further geochemical investigations of host sediments. At Holzmaden,
666 the majority of the ichthyosaur fossil record stretches from epsilon II₁ to epsilon II₁₀,
667 which corresponds to a large interval encompassing periods before, within and after
668 the T-OAE (Maxwell & Vincent, 2016). Most of the Posidonia Shale facies in SW
669 Germany consist of bituminous shales: the occurrence of carbonate concretions is
670 reported from epsilon II₄, but most Toarcian ichthyosaurs from the Holzmaden area
671 are preserved as flattened skeletons from the bituminous shale. Therefore, putting
672 efforts into prospecting for marine vertebrates from nodular carbonate concretions of
673 the T-OAE, notably in the level corresponding to the upper portion of epsilon II₄, will
674 likely yield specimens preserved in volume, including soft tissues. Such a prospect is
675 particularly appealing because the anatomical organization of internal soft organs is
676 virtually unknown in ichthyosaurs and other marine reptiles of that age.

677

678 **Early Jurassic evolution of ichthyosaurs in relation to the T-OAE.** The youngest
679 ichthyosaur skeleton from the LafargeHolcim Val d’Azergues quarry is
680 *Temnodontosaurus azerguensis* from the base of the *bifrons* Zone, which is post-T-
681 OAE. Here, we report stenopterygiids both within (base of *serpentinum* Zone) and
682 after (middle of *serpentinum* Zone) the negative carbon isotopic excursion of the T-
683 OAE. The T-OAE initiates near the limit of the *tenuicostatum* - *serpentinum* zones
684 (Fig. 2). The oldest occurrence of the genus *Stenopterygius* has been recorded from
685 epsilon I₂ level in Germany (Maxwell 2012), which corresponds to the base of the
686 *tenuicostatum* zone. This suggests that *Stenopterygius* was already present just before
687 the T-OAE. In SW Germany, *Stenopterygius* is particularly abundant in epsilon II₃
688 level (Maxwell 2012), i.e. the top of the *tenuicostatum* zone, which corresponds to the
689 onset of the T-OAE. Bottom anoxic conditions are ideal to preserve marine faunas
690 and this may explain the abundance of marine vertebrates preserved as complete
691 skeletons from this lower Toarcian interval (Ulrichs *et al.* 1994). Marine vertebrates
692 from the Toarcian of Yorkshire are equally abundant and finely preserved in
693 bituminous shales within the *falciferum* subzone (Benton & Taylor 1984). Benton &
694 Taylor (1984) state that the German fauna is older than the Yorkshire fauna, and a
695 *falciferum* subzone for the Yorkshire fauna indicates that this marine assemblage is
696 post-T-OAE. Ilminster specimens from the ‘saurian and fish bed’ are preserved in
697 carbonate concretions collected from the *exaratum* subzone (Williams *et al.* 2015),
698 which corresponds to the level that yielded the presently described carbonate
699 concretion from Beaujolais containing the ichthyosaur specimen (MHNL 20103364).
700 The carbonate concretion with the nicely preserved ichthyosaur from Curcy/La Caïne
701 in Normandy comes from the *serpentinum* Zone, else known as the “Argiles à
702 poissons” (Mazin 1988) but more precise stratigraphic details are unknown. Another
703 nice skull preserved in volume (NHMUK PV OR 33157) comes from Curcy in
704 Normandy and was originally mentioned and figured by Owen (1849) and by Caine &
705 Benton (2011). Marine reptile discoveries from Belgium and Luxembourg were
706 mostly recorded from the *serpentinum* Zone, *exaratum* subzone (Godefroit 1994).
707 With the onset of the T-OAE, marine life experienced a major environmental
708 perturbation with a well-documented impact on the invertebrate fauna (Little &
709 Benton 1995; Harries & Little 1999; Macchioni & Cecca 2002; Wignall *et al.* 2005;
710 Suan *et al.* 2008; Caswell *et al.* 2009). Although recent studies do not validate an
711 extinction of marine vertebrates during the T-OAE (Vincent *et al.* 2013), it was

712 statistically demonstrated that ichthyosaur body size was impacted (Maxwell &
713 Vincent 2016). The rich fossil record from the Holzmaden area shows that the most
714 recent levels of the *serpentinum* Zone contain the largest known specimens of the
715 genus *Stenopterygius* (Maxwell & Vincent 2016) as well as the oldest known records
716 of *Suevoleviathan*. The long skull of MHNL 20103062 (< 60 cm) and its stratigraphic
717 position within the middle levels of the *serpentinum* Zone are consistent with these
718 observations. The largest *Stenopterygius* specimens from Germany have a skull length
719 of 72 cm for *S. uniter*, 67 cm for *S. triscissus* and 56 cm for *S. quadriscissus* (Maxwell
720 & Vincent 2016). The Posidonia Shale has yielded hundreds if not thousands of
721 vertebrate specimens, and indeed provides an ideal context to run such quantitative
722 diversity analyses, but the impact of the T-OAE on marine faunas can be studied
723 further elsewhere, contextualizing the fossil record with precisely dated occurrences,
724 thanks to its apparent wide extension across Europe and also globally (Martindale *et*
725 *al.* 2017).

726 Pre-T-OAE vertebrate fossils are important to understand marine diversity
727 change in relation to the environmental perturbation of the Toarcian. For example, an
728 apparent turnover can be identified between ‘Lower Liassic’ and ‘Upper Liassic’
729 ichthyosaur faunas (Hungerbühler & Sachs 1996), but growing evidence supports this
730 turnover occurring in the Pliensbachian. During the Toarcian, *Stenopterygius* is the
731 most abundant genus and seems to be the ecomorphological equivalent of the
732 Pliensbachian genera *Ichthyosaurus* and *Leptonectes*. The youngest stratigraphically
733 constrained occurrences of *Ichthyosaurus* are from the lower Pliensbachian strata of
734 the UK (Lomax & Massare 2015; Massare & Lomax 2016); the youngest constrained
735 records of *Leptonectes* are also from the lower Pliensbachian (*L. moorei* from the UK
736 and more fragmentary remains attributable to *Leptonectes* from the UK, Belgium,
737 Spain, and SW Germany: Fraas 1892 [see Maisch 2010]; Godefroit 1992; Fernández
738 *et al.* 2018, McGowan & Milner 1999; Lomax & Massare 2018). The upper
739 Pliensbachian specimen previously referred to *Leptonectes* (Maisch & Reisdorf 2006)
740 has been reinterpreted as *Hauffiopteryx*, a genus best-documented from the Toarcian
741 (Maxwell & Cortés 2020). An ischiopubis from the early-middle Liassic of the UK,
742 cited by some authors as the earliest occurrence of *Stenopterygius* (McGowan 1978;
743 Hungerbühler & Sachs 1996), is inconsistent with the Toarcian representatives of this
744 genus based on the posteromedial orientation and large size of the obturator foramen,
745 and incomplete lateral fusion between the ischium and pubis (McGowan 1978: pl.

746 2.3). As stated above, the occurrence of *Stenopterygius* in lowermost Toarcian strata
747 (Maxwell 2012; Maxwell & Vincent 2016; this study) suggests that this genus was
748 already present before the depositional record of the T-OAE started. Additional
749 confusion in the distribution of Early Jurassic ichthyosaurs is caused by taxonomic
750 identifications with a number of historical finds having been attributed to
751 *Leptopterygius* von Huene 1922, a now obsolete genus name, which encompassed the
752 different genera *Leptonectes*, *Suevoleviathan* and *Temnodontosaurus*. The
753 Pliensbachian ichthyosaur record is poor and essentially originates from the lowest
754 levels. Further sampling of this interval is important to understand evolutionary
755 patterns during the Early Jurassic.

756

757 **Conclusions**

758

759 Our study highlights some future directions of research in order to clarify our
760 understanding of faunal evolution in relation to a major environmental perturbation,
761 i.e. testing the effects of the T-OAE on marine vertebrates, especially outside of the
762 well-studied southwest German basin.

763 An apparent faunal transition may have occurred between lower Pliensbachian
764 and Toarcian ichthyosaur assemblages. However, upper Pliensbachian strata are
765 undersampled and the timing of this transition cannot be constrained yet. Whether the
766 T-OAE may represent an abiotic influence as to the replacement of Pliensbachian
767 ichthyosaurs by Toarcian ones seems unlikely considering that pre-T-OAE
768 ichthyosaurs are apparently already represented by the genus *Stenopterygius*. This
769 requires a precise stratigraphic and taxonomic context for each fossil individual to be
770 recorded.

771 The taxonomy of Lower Jurassic ichthyosaurs is in critical need of a revision
772 and several taxa may be synonymous. Despite numerous recent efforts (e.g. Lomax &
773 Massare 2015; Maxwell & Cortés 2020), differences between *Leptonectes* and
774 *Stenopterygius* are tenuous and ichthyosaur diversity may have been overlooked in a
775 number of cases that still need to be identified. If Pliensbachian and Toarcian
776 ichthyosaur faunas are homogeneous, then the impact of the T-OAE on these faunas
777 remains minimal and an explanation of what triggered this faunal transition is still
778 required.

779 Finally, we emphasize that the study of nodular carbonate concretions might

780 reveal important information about soft tissue preservation, including the preservation
781 of organs in three dimensions. As concerns marine vertebrates, this could correspond
782 to a major advance to better understand the palaeobiology of these extinct animals and
783 the adaptations of tetrapods from terrestrial to marine environments. Multidisciplinary
784 approaches, such as that proposed in this work combining palaeontology,
785 sedimentology and chemostratigraphy shall provide a solid framework to finely track
786 the impact of environmental changes on marine vertebrates on both short- and long-
787 term timescales. As an example, renewed field efforts can be directed at historical
788 localities (e.g. La Caine or Strawberry Bank) that yielded exquisitely preserved
789 specimens but where a detailed stratigraphic framework is lacking.

790

791 We thank all the Association Paleorhodania volunteers involved in the field seasons (2009–2013) as
792 well as the members of the Association Geopaleo, the LafargeHolcim Val d’Azergues quarry, Espace
793 Pierres Folles, Musée des Confluences de Lyon, Laboratoire de Géologie de Lyon and CNRS INSU.
794 Special thanks to Didier Berthet, Jean Arbault, Didier Genissel, Thierry Fuentes and Bertrand Leopardo
795 for their continuous support all along this project. François Fourel, Laurent Simon and Philippe Telouk
796 are thanked for their help with isotope analyses. JS was partly supported by research grants APVV 17-
797 0555 and VEGA 2/0169/19. We thank the editor Matías Reolid as well as Michael Benton and one
798 anonymous reviewer for their comments that improved the content of this work.

799

800 **References**

801

802 Anderson, K. L., Druckenmiller, P. S., Erickson, G. M. & Maxwell, E. E. 2018.
803 Skeletal microstructure of *Stenopterygius quadriscissus* (Reptilia, Ichthyosauria) from
804 the Posidonienschiefer (Posidonia Shale, Lower Jurassic) of Germany. *Palaeontology*,
805 **62**, 433–449.

806

807 Angino, E. E., Billings, G.K., Andersen, N. 1966. Observed variations in the
808 strontium concentration of sea water. *Chemical Geology*, **1**, 145–153.

809

810 Ansoerge, J. 2003. Insects from the Lower Toarcian of Middle Europe and England.
811 *Acta zoologica cracoviensia*, **46**, 291–310.

812

813 Bécaud, M. 2006. Les Harpoceratinae, Hildoceratinae et Paroniceratinae du Toarcien
814 de la Vendée et des Deux-Sèvres (France). Documents des Laboratoires de Géologie
815 de Lyon, 162, 245 p.
816

817 Benton, M. J. & Taylor, M. A. 1984. Marine reptiles from the Upper Lias (Lower
818 Toarcian, Lower Jurassic) of the Yorkshire Coast. *Proceedings of the Yorkshire*
819 *Geological Society*, **44**, 399–429.
820

821 Benton, M. J. & Spencer, P. S. 1995. Fossil reptiles of Great Britain. Springer Science
822 and Business Media, 386 pp.
823

824 de Blainville, H. D. 1835. Description de quelques espèces de reptiles de la
825 Californie, précédée de l'analyse d'un système général d'Erpétologie et
826 d'Amphibiologie. *Nouvelles Annales du Muséum d'Histoire Naturelle, Paris*, **4**, 233–
827 295.
828

829 Böttcher, R. 1989. Über die Nahrung eines *Leptopterygius* (Ichthyosauria, Reptilia)
830 aus dem süddeutschen Posidonienschiefer (Unterer Jura) mit Bemerkungen über den
831 Magen der Ichthyosaurier. *Stuttgarter Beiträge zur Naturkunde Serie B (Geologie und*
832 *Paläontologie)*, **155**, 1–19.
833

834 Böttcher, R. 1990. Neue Erkenntnisse über die Fortpflanzungsbiologie der
835 Ichthyosaurier. *Stuttgarter Beiträge zur Naturkunde B*, **164**, 1–51.
836

837 Caine, H. & Benton, M. J. 2011. Ichthyosauria from the Upper Lias of Strawberry
838 Bank, England. *Palaeontology*, **54**, 1069–1093.
839

840 Dick, D. & Maxwell, E. E. 2015. Ontogenetic tooth reduction in *Stenopterygius*
841 *quadriscissus* (Reptilia: Ichthyosauria): negative allometry, changes in growth rate,
842 and early senescence of the dental lamina. *PLoS ONE*, **10**, e0141904.
843

844 Dick, D., Schweigert, G. & Maxwell, E. E. 2016. Trophic niche ontogeny and
845 palaeoecology of early Toarcian *Stenopterygius* (Reptilia: Ichthyosauria).
846 *Palaeontology*, **59**, 423–431.

847

848 Elmi, S., Rulleau, L., Gabilly, J. & Mouterde, R. 1997. Toarcien. In: Cariou, E. &
849 Hantzpergue, P. (coord.) Biostratigraphie du Jurassique ouest-européen et
850 méditerranéen: zonations parallèles et distribution des invertébrés et microfossiles.
851 *Bulletin Centre Recherches Elf Exploration Production, Mémoire*, **17**, 25–36.

852

853 Fernández, M. 1994. A new long-snouted ichthyosaur from the early Bajocian of
854 Neuquen Basin (Argentina). *Ameghiniana*, **31**, 291–297.

855

856 Fernández, M., Archuby, F., Talevi, M. & Ebner, R. 1994. Ichthyosaurian eyes:
857 paleobiological information content in the sclerotic ring of *Caypullisaurus*
858 (Ichthyosauria, Ophthalmosauria). *Journal of Vertebrate Paleontology*, **25**, 330–337.

859

860 Fernández, M. S., Piñuela, L. & García-Ramos, J. C. 2018. First report of *Leptonectes*
861 (Ichthyosauria: Leptonectidae) from the Lower Jurassic (Pliensbachian) of Asturias,
862 northern Spain. *Palaeontologia Electronica*, **21.2.29A**, 1–15.

863

864 Fischer, V., Guiomar, M. & Godefroit, P. 2011. New data on the palaeobiogeography
865 of Early Jurassic marine reptiles: the Toarcian ichthyosaur fauna of the Vocontian
866 Basin (SE France). *Neues Jahrbuch für Geologie und Paläontologie-Abhandlungen*,
867 **261**, 111–127.

868

869 Fraas, E. 1888. Ueber die Finne von Ichthyosaurus. Jahreshefte des vereins für
870 vaterländische. Naturkunde. Württemberg 44, 280–303.

871

872 Fraas, E. 1892. *Ichthyosaurus numismalis* E. Fraas. *Jahreshefte des Vereins für*
873 *vaterländische Naturkunde in Württemberg*, **48**, 22–31.

874

875 Fraas, E. 1913. Ein unverdrückter Ichthyosaurus-Schädel. *Mitteilungen aus dem K.*
876 *Naturalienkabinett*, **79**, 1–12.

877

878 Godefroit, P. 1992. Présence de *Leptopterygius tenuirostris* (Reptilia, Ichthyosauria)
879 dans le Lias moyen de Lorraine belge. *Bulletin de L'Institut Royal des Sciences*
880 *Naturelles de Belgique, Sciences de la Terre*, **62**, 163–170.

881

882 Godefroit, P. 1994. *Les reptiles marins du Toarcien (Jurassique inférieur) belgo-*
883 *luxembourgeois* (No. 39). Service géologique de Belgique.

884

885 Hauff, B. 1921. Untersuchung der Fossilfundstätten von Holzmaden im
886 Posidonienschiefer des Oberen Lias Württembergs. *Palaeontographica*, **64**, 1–42.

887

888 Hauff, R. B., Heunisch, C., Hochsprung, U., Ilger, J.-M., Joger, U., Klopschar, M.,
889 Kosma, R., Krüger, F. J., Thies, D. & Zellmer, H. 2017. *Jurameer: Niedersachsens*
890 *versunkene Urwelt*. Munich: Verlag Dr. Fritz Pfeil.

891

892 Heller, W. 1966. Untersuchungen zur sogenannten Hauterhaltung bei Ichthyosauriern
893 aus dem Lias epsilon Holzmadens (Schwaben). *Neues Jahrbuch für Mineralogie,*
894 *Monatshefte*, **5**, 304–317.

895

896 Hofmann, J. 1958. Einbettung und Zerfall der Ichthyosaurier im Lias von Holzmaden.
897 *Meyniana*, **6**, 10–55.

898

899 von Huene, F. 1931. Neue Studien über Ichthyosaurier aus Holzmaden.
900 *Abhandlungen der Senckenbergischen naturforschenden Gesellschaft*, **42**, 345–382.

901

902 Hungerbühler, A. & Sachs, S. 1996. Ein grosser Ichthyosaurier aus dem
903 Pliensbachium von Bielefeld: neue Einblicke in die Ichthyosaurier des mittleren Lias
904 und das Gebiss von *Temnodontosaurus*. *Bericht Naturwissenschaftlicher Verein für*
905 *Bielefeld und Umgegend*, **37**, 15–52.

906

907 Jäger, M. 2005. *The museum of fossils in the Werkforum: Guidebook of the exhibition*
908 *of Jurassic fossils*, 3rd edn. Dotternhausen: Holcim.

909

910 Jaekel, O. 1904. Eine neue Darstellung von *Ichthyosaurus*. *Zeitschrift der Deutschen*
911 *Geologischen Gesellschaft*, **56**, 26–34.

912

913 Ji, C., Jiang, D. -Y., Motani, R., Rieppel, O., Hao, W. & Sun, Z.-Y. 2016. Phylogeny
914 of the Ichthyopterygia incorporating recent discoveries from South China. *Journal of*

915 *Vertebrate Paleontology*, **36**, e1025956.

916

917 Keller, T. 1992. "Weichteil-Erhaltung" bei großen Vertebraten (Ichthyosauriern) des
918 Posidonienschiefers Holzmadens (Oberer Lias, Mesozoikum Süddeutschlands).
919 *Kaupia: Darmstädter Beiträge zur Naturgeschichte*, **1**, 23–62.

920

921 Lindgren, J., Sjövall, P., Thiel, V., Zheng, W., Ito, S., Wakamatsu, K., Hauff, R.,
922 Kear, B. P., Engdahl, C., Eriksson, M. E., Jarenmark, M., Sachs, S., Ahlberg, P. E.,
923 Marone, F., Kuriyama, T., Gustafsson, O., Malmberg, P., Thomen, A., Rodríguez-
924 Meizoso, I., Uvdal P., Ojika, M. & Schweitzer, M. H. 2018. Soft-tissue evidence for
925 homeothermy and crypsis in a Jurassic ichthyosaur. *Nature*, **564**, 359–365.

926

927 Lingham-Soliar, T. 1999. Rare soft tissue preservation showing fibrous structures in
928 an ichthyosaur from the Lower Lias (Jurassic) of England. *Proceedings of the Royal*
929 *Society of London B*, **266**, 2367–2373.

930

931 Little, C. T. & Benton, M. J. 1995. Early Jurassic mass extinction: a global long-term
932 event. *Geology*, **23**, 495–498.

933

934 Lomax, D. R. & Massare, J. A. 2015. A new species of *Ichthyosaurus* from the Lower
935 Jurassic of West Dorset, England, U.K. *Journal of Vertebrate Paleontology*, **35**,
936 e903260.

937

938 Lomax, D. R. & Massare, J. A. 2018. A forefin of *Leptonectes* from the Lower
939 Jurassic (Pliensbachian) of Dorset, UK. *Proceedings of the Geologists' Association*,
940 **129**, 770–773.

941

942 Lomax, D. R., Evans, M. & Carpenter, S. 2018. An ichthyosaur from the UK Triassic-
943 Jurassic boundary: a second specimen of the leptonectid ichthyosaur *Wahlisaurus*
944 *massarae* Lomax 2016. *Geological Journal*, **2018**, 1–8.

945

946 Lomax, D. R., Massare, J. A. & Evans, M. 2020. New information on the skull roof of
947 *Protoichthyosaurus* (Reptilia: Ichthyosauria) and intraspecific variation in some
948 dermal skull elements. *Geological Magazine*, **157**, 640–650.

949

950 Maisch, M. W. 1998a. Kurze Übersicht der Ichthyosaurier des Posidonienschiefers
951 mit Bemerkungen zur Taxonomie der Stenopterygiidae und Temnodontosauridae.
952 *Neues Jahrbuch für Geologie und Paläontologie Abhandlungen*, **209**, 401–431.

953

954 Maisch, M. W. 1998b. A new ichthyosaur genus from the Posidonia Shale (Lower
955 Toarcian, Jurassic) of Holzmaden, SW Germany with comments on the phylogeny of
956 post-Triassic ichthyosaurs. *Neues Jahrbuch für Geologie und Paläontologie*
957 *Abhandlungen*, **209**, 47–78.

958

959 Maisch, M. W. 2001. Neue Exemplare der seltenen Ichthyosauriergattung
960 *Suevoleviathan* Maisch 1998 aus dem Unteren Jura von Südwestdeutschland.
961 *Geologica et Palaeontologica*, **35**, 145–160.

962

963

964 Maisch, M. W. & Matzke, A. T. 2000. The Ichthyosauria. *Stuttgarter Beiträge zur*
965 *Naturkunde: Serie B Geologie und Paläontologie*, **298**, 1–159.

966

967 Maisch, M. W. & Matzke, A. T. 2003. The cranial osteology of the ichthyosaur
968 *Leptonectes* cf. *tenuirostris* from the Lower Jurassic of England. *Journal of*
969 *Vertebrate Paleontology*, **23**, 116–127.

970

971 Maisch, M. W. & Ansorge, J. 2004. The Liassic ichthyosaur *Stenopterygius* cf.
972 *quadriscissus* from the lower Toarcian of Dobbertin (northeastern Germany) and
973 some considerations on lower Toarcian marine reptile palaeobiogeography.
974 *Paläontologische Zeitschrift*, **78**, 161–171.

975

976 Maisch, M. W. & Reisdorf, A. G. 2006. Evidence for the longest stratigraphic range
977 of a post-Triassic ichthyosaur: a *Leptonectes tenuirostris* from the Pliensbachian
978 (Lower Jurassic) of Switzerland. *Geobios*, **39**, 491–505.

979

980 Maisch, M. W. 2008. Revision der Gattung *Stenopterygius* Jaekel, 1904 emend. von
981 Huene, 1922 (Reptilia: Ichthyosauria) aus dem unteren Jura Westeuropas.
982 *Paleodiversity*, **1**, 227–271.

983

984 Maisch, M. W. 2010. Phylogeny, systematics, and origin of the Ichthyosauria – the
985 state of the art. *Palaeodiversity*, **3**, 151–214.

986

987 Marek, R. D., Moon, B. C., Williams, M. & Benton, M. J. 2015. The skull and
988 endocranium of a Lower Jurassic ichthyosaur based on digital reconstructions.

989 *Palaeontology*, **58**, 723–742.

990

991 Martin, J. E., Fischer, V., Vincent, P. & Suan, G. 2012. A longirostrine

992 *Temnodontosaurus* (Ichthyosauria) with comments on Early Jurassic ichthyosaur
993 niche partitioning and disparity. *Palaeontology*, **55**, 995–1005.

994

995 Martindale, R. C., Them II, T. R., Gill, B. C., Marroquín, S. M. & Knoll, A. H. 2017.
996 A new Early Jurassic (ca. 183 Ma) fossil Lagerstätte from Ya Ha Tinda, Alberta,
997 Canada. *Geology*, **45**, 255–258.

998

999 Martill, D. M. 1993. Soupy substrates: a medium for the exceptional preservation of
1000 ichthyosaurs of the Posidonia Shale (Lower Jurassic) of Germany. *Kaupia*, **2**, 77–97.

1001

1002 Martill, D. M. 1995. An ichthyosaur with preserved soft tissue from the Sinemurian of
1003 southern England. *Palaeontology*, **38**, 897–903.

1004

1005 Massare, J. A. & Lomax, D. R. 2016. A new specimen of *Ichthyosaurus conybeari*
1006 (Reptilia: Ichthyosauria) from Watchet, Somerset, England, U.K., and a reexamination
1007 of the species. *Journal of Vertebrate Paleontology*, **36**, e1163264.

1008

1009 Maxwell, E. E. 2012. New metrics to differentiate species of *Stenopterygius* (Reptilia:
1010 Ichthyosauria) from the Lower Jurassic of southwestern Germany. *Journal of*
1011 *Paleontology*, **86**, 105–115.

1012

1013 Maxwell, E. E. & Cortés, D. 2020. A revision of the Early Jurassic ichthyosaur
1014 *Hauffiopteryx* (Reptilia: Ichthyosauria), and description of a new species from
1015 southwestern Germany. *Palaeontologia Electronica*, **23**, a31. doi.org/10.26879/937

1016

1017 Maxwell, E. E., Fernández, M. S. & Schoch, R. 2012. First diagnostic marine reptile
1018 remains from the Aalenian (Middle Jurassic): a new ichthyosaur from Southwestern
1019 Germany. *PLoS ONE*, **7**, e41692.

1020

1021 Maxwell, E. E. & Vincent, P. 2016. Effects of the early Toarcian Oceanic Anoxic
1022 Event on ichthyosaur body size and faunal composition in the Southwest German
1023 Basin. *Paleobiology*, **42**, 117–126.

1024

1025 Maxwell, E. E. 2018. Redescription of the ‘lost’ holotype of *Suevoleviathan integer*
1026 (Bronn, 1844) (Reptilia: Ichthyosauria). *Journal of Vertebrate Paleontology*, **38**,
1027 e1439833.

1028

1029 Mazin, J. M. 1988. Le crâne d’*Ichthyosaurus tenuirostris* Conybeare, 1822 (Toarcien,
1030 La Caine, Normandie, France). *Bulletin de la Société linnéenne de Normandie*, 112–
1031 **113**, 121–132.

1032

1033 McArthur, J. M., Donovan, D. T., Thirwall, M. F., Fouke, B. W. & Matthey, D. 2000.
1034 Strontium isotope profile of the early Toarcian (Jurassic) oceanic anoxic event, the
1035 duration of ammonite biozones, and belemnite palaeotemperatures. *Earth and*
1036 *Planetary Science Letters*, **179**, 269–285.

1037

1038 McArthur, J. M., Howarth, R. J. & Bailey, T. R. 2001. Strontium Isotope
1039 Stratigraphy: LOWESS Version 3 : best fit to the marine Sr-isotope curve for 0–509
1040 Ma and accompanying look-up table for deriving numerical age. *The Journal of*
1041 *Geology*, **109**, 155–170.

1042

1043 McArthur, J. M., Page, K., Duarte, L. V., Thirlwall, M. F., Li, Q., Weis, R. & Comas-
1044 Rengifo, M. J. 2020. Sr-isotope stratigraphy ($^{87}\text{Sr}/^{86}\text{Sr}$) of the lowermost Toarcian of
1045 Peniche, Portugal, and its relation to ammonite zonations. *Newsletters on*
1046 *Stratigraphy*, **53**, 297–312.

1047

1048 McGowan, C. 1978. Further evidence for the wide geographical distribution of
1049 ichthyosaur taxa (Reptilia: Ichthyosauria). *Journal of Paleontology*, **52**, 1155–1162.

1050

1051 McGowan, C. 1979. A revision of the lower Jurassic ichthyosaurs of Germany with
1052 descriptions of two new species. *Palaeontographica Abteilung A*, **166**, 93–135.
1053

1054 McGowan, C. 1994. *Temnodontosaurus risor* is a juvenile of *T. platyodon* (Reptilia:
1055 Ichthyosauria). *Journal of Vertebrate Paleontology*, **14**, 472–479.
1056

1057 McGowan, C. & Milner, A. C. 1999. A new Pliensbachian ichthyosaur from Dorset,
1058 England. *Palaeontology*, **42**, 761–768.
1059

1060 McGowan, C., & Motani, R. 2003. Handbook of Paleoherpertology, Part 8
1061 Ichthyopterygia. *Verlag Dr. Friedrich Pfeil, Munich*, 175.
1062

1063 Motani, R. 1999. Phylogeny of the Ichthyopterygia. *Journal of Vertebrate*
1064 *Paleontology*, **19**, 473–496.
1065

1066 Motani, R. 2005. True skull roof configuration of *Ichthyosaurus* and *Stenopterygius*
1067 and its implications. *Journal of Vertebrate Paleontology*, **25**, 338–342.
1068

1069 Muscente, A. D., Schiffbauer, J. D., Broce, J., Laflamme, M., O'Donnell, K., Boag, T.
1070 H., Meyer, M., Hawkins, A. D., Huntley, J. W., McNamara, M., MacKenzie, L. A.,
1071 Stanley Jr., G. D., Hinman, N. W., Hofmann, M. H. & Xiao, S. 2017. Exceptionally
1072 preserved fossil assemblages through geologic time and space. *Gondwana Research*,
1073 **48**, 164–188.
1074

1075 Owen, R. 1849. A history of British fossil reptiles. Vol. III. London: Cassell and
1076 Company Limited.
1077

1078 Page, K. 2003. The Lower Jurassic of Europe: its subdivision and correlation.
1079 *Geological Survey of Denmark and Greenland Bulletin*, **1**, 23–59.
1080

1081 Plet, C., Grice, K., Pagès, A., Verrall, M., Coolen, M. J. L., Ruebsam, W., Rickard,
1082 W. D. A., Schwark, L. 2017. Palaeobiology of red and white blood cell-like
1083 structures, collagen and cholesterol in an ichthyosaur bone. *Scientific Reports*, **7**,
1084 13776.

1085
1086 Quenstedt, F. A. 1856-1858. Der Jura. VI + 842 S., Tübingen (H. Laupp).
1087
1088 Raiswell, R. 1988. Chemical model for the origin of minor limestone-shale cycles by
1089 anaerobic methane oxidation. *Geology*, **16**, 641–644.
1090
1091 Reisdorf, A.G., Maisch, M.W. & Wetzel, A. 2011. First record of the leptonectid
1092 ichthyosaur *Eurhinosaurus longirostris* from the Early Jurassic of Switzerland and its
1093 stratigraphic framework. *Swiss Journal of Geosciences*, **104**, 211–224.
1094
1095 Riegraf, W., Werner, G. & Lörcher, F. 1984. Der Posidonienschiefer.
1096 Biostratigraphie, Fauna und Fazies des südwestdeutschen Untertoarciums (Lias ε).
1097 Stuttgart: Ferdinand Enke.
1098
1099 Röhl, H.-S., Schmid-Röhl, A., Oschmann, W., Frimmel, A. & Schwark, L. 2001. The
1100 Posidonia Shale (Lower Toarcian) of SW-Germany: an oxygen-depleted ecosystem
1101 controlled by sea level and palaeoclimate. *Palaeogeography, Palaeoclimatology,*
1102 *Palaeoecology*, **165**, 27–52.
1103
1104 Rulleau, L. 2006. Biostratigraphie et paléontologie du Lias supérieur et du Dogger de
1105 la région lyonnaise. Section Géologie et Paléontologie du Comité d'Entreprise Lafarge
1106 Ciments, 382 p.
1107
1108 Stumpf, S. 2016. New information on the marine reptile fauna from the lower
1109 Toarcian (Early Jurassic) “Green Series” of North-Eastern Germany. *Neues Jahrbuch*
1110 *für Geologie und Paläontologie, Abhandlungen*, **280**, 87–105.
1111
1112 Suan, G., Rulleau, L., Mattioli, E., Suchéras-Marx, B., Rousselle, B., Pittet, B.,
1113 Vincent, P., Martin, J. E., Léna, A., Spangenberg, J. E. & Föllmi, K.B. 2013.
1114 Palaeoenvironmental significance of Toarcian black shales and event deposits from
1115 southern Beaujolais, France. *Geological Magazine*, **150**, 728–742.
1116
1117 Urlichs, M. von, Wild, R. & Ziegler, B. 1994. Der Posidonien-Schiefer des unteren
1118 Juras und seine Fossilien. *Stuttgarter Beiträge zur Naturkunde, Serie C*, **36**, 1–95.

1119

1120 Vincent, P., Martin, J.E., Fischer, V., Suan, G., Khalloufi, B., Suchéras-Marx, B.,
1121 Léna, A., Janneau, K., Rousselle, B. & Rulleau, L. 2013. Marine vertebrate remains
1122 from the Toarcian–Aalenian succession of southern Beaujolais, Rhône, France.
1123 *Geological Magazine*, **150**, 822–834.

1124

1125 Vincent, P., Weis, R., Kronz, G. & Delsate, D. 2019 *Microcleidus melusinae*, a
1126 new plesiosaurian (Reptilia, Plesiosauria) from the Toarcian of Luxembourg.
1127 *Geological Magazine*, **156**, 99–116.

1128

1129 Williams, M., Benton, M. J. & Ross, A. 2015. The strawberry bank Lagerstätte
1130 reveals insights into early Jurassic life. *Journal of the Geological Society*, **172**, 683–
1131 692.

1132

1133 **Figure captions**

1134

1135 **Fig. 1.** Photographs of the Belmont d’Azergues LafargeHolcim Val d’Azergues
1136 quarry, Beaujolais, France, taken during the 2013 fieldwork and contextualizing the
1137 area of discovery of *Stenopterygius* sp. remains described in this work. (a), general
1138 view of the quarry looking South from the hardground surface of the *variabilis* zone;
1139 (b), looking North, view of the trench realized through the *serpentinum* Zone where
1140 both *Stenopterygius* sp. finds were made; (c), aerial view (Googlemap) of the quarry
1141 identifying the areas of the inset photographs A and B.

1142

1143 **Fig. 2.** Lithological, biostratigraphic and geochemical data from Toarcian strata of (a)
1144 LafargeHolcim Val d’Azergues quarry in SE France and (b), Dotternhausen in SW
1145 Germany. The green band marks the interval of lowest carbon isotope values, i.e., the
1146 core of the negative carbon isotope excursion associated with the Toarcian Oceanic
1147 Anoxic Event. The stratigraphic position of ichtthyosaur specimens discussed in the
1148 text is indicated along the lithological log. The sedimentary matrix of the large
1149 carbonate concretion found during the excavation of the trench in the basal 2.5 m
1150 interval yielded a $\delta^{13}\text{C}_{\text{carb}}$ value of -3.88% . Comparatively low values are only
1151 recorded in the interval comprised between 0.2 and 0.5 m, enabling to narrow down
1152 its likely provenance. Correlations between the two sites were established using litho-,

1153 bio- and chemostratigraphic features. Data for LafargeHolcim Val d’Azergues quarry
1154 from this study and Suan *et al.* (2013). Data for Dotternhausen from Bailey *et al.*
1155 (2003) and Suan *et al.* (2015). Epsilon levels from Hauff (1921) and Röhl *et al.*
1156 (2001).

1157

1158 **Fig. 3.** Photograph (a) and drawing (b) of the left lateral side of the skull of (MHNL
1159 20103062) *Stenopterygius* sp. from the Toarcian of Beaujolais. Abbreviations: en,
1160 external nares; for, foramen; fr, frontal; iff, interfrontal foramen; ju, jugal; la, lacrimal;
1161 lac. sut., lacrimal suture; mx, maxilla; p, parietal; pfr, prefrontal; pif, pineal foramen;
1162 pmx, premaxilla; pof, postfrontal; qj, quadratojugal; sr, sclerotic ring; t, teeth. [Full
1163 page width]

1164

1165 **Fig. 4.** Isolated tooth of *Stenopterygius* sp. (MHNL 20103062) from the Toarcian of
1166 Beaujolais in labial or lingual (a, b), mesial or distal (c, d) and basal (e) views. [Full
1167 page width]

1168

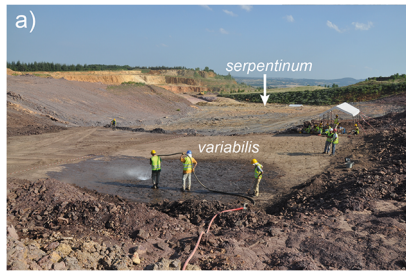
1169 **Fig. 5.** The nodular concretion (MHNL 20103364) (a) as recovered during fieldwork
1170 with * corresponding to (b), articulated phalanges; ** corresponding to (c), anterior
1171 tip of the rostrum with arrows corresponding to teeth in section; and ***
1172 corresponding to (d), section through the rib cage showing ribs and gastralia (arrows)
1173 delimiting an internal zone of purple hue suspected of representing oxidized organic
1174 matter together with close-ups (not to scale) of the purple hue within sediment (e) and
1175 around gastralia (f). Abbreviations: c, centrum; ga, gastralia. [Full page width]

1176

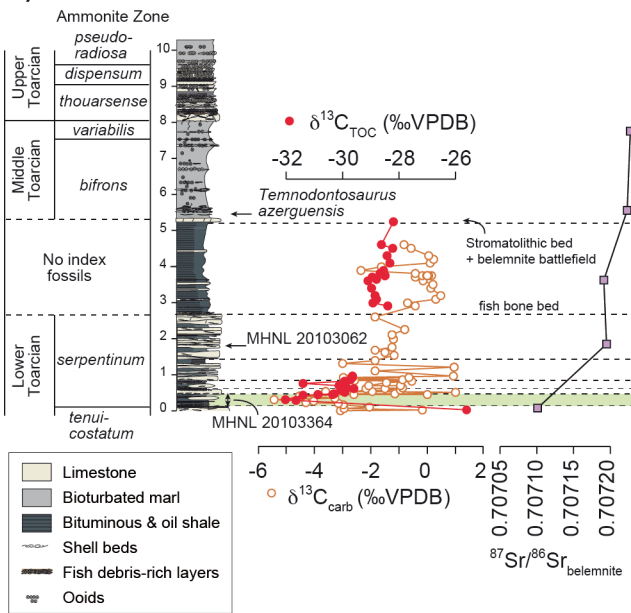
1177 Table 1. List of early Toarcian localities with ichthyosaur-bearing carbonate
1178 concretions (AZ = Ammonite Zone).

1179

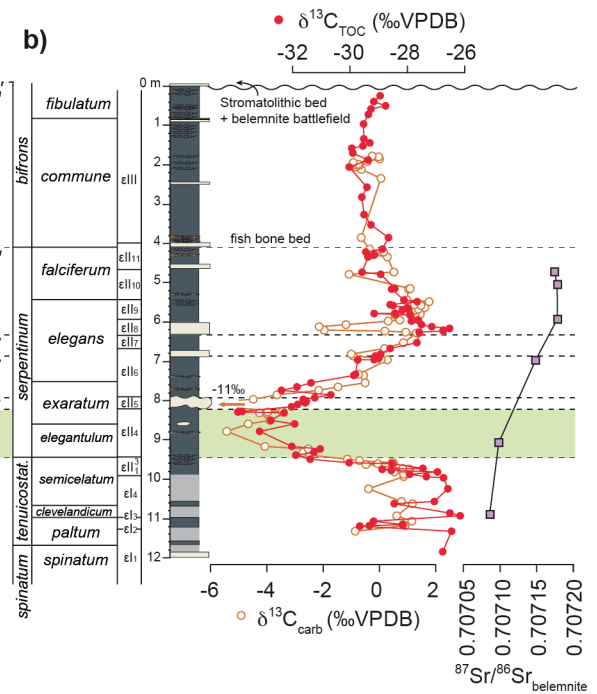
1180 Supplementary Data. Geochemical dataset used in the present study including bulk
1181 sediment inorganic and organic carbon isotope composition ($\delta^{13}\text{C}$) and radiogenic
1182 strontium isotope ($^{87}\text{Sr}/^{86}\text{Sr}$) values of belemnites.



a)

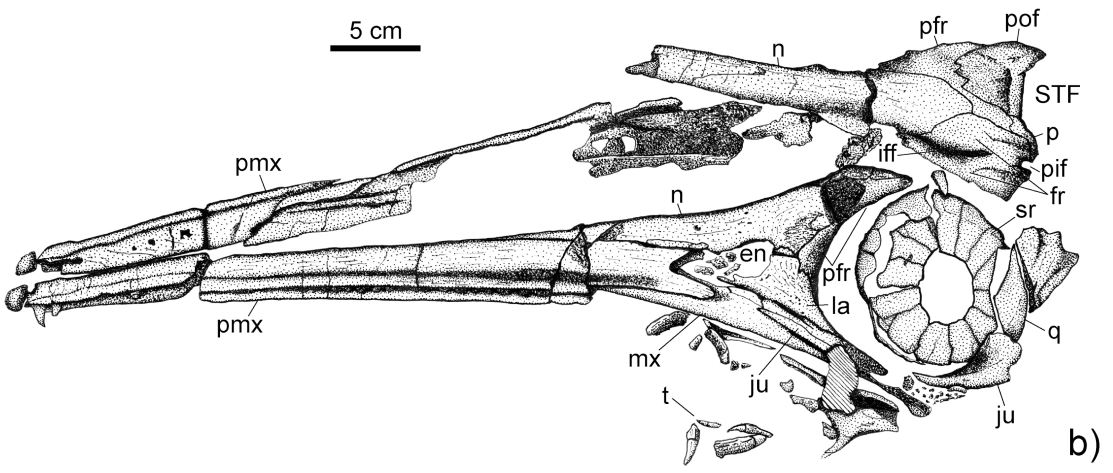


b)

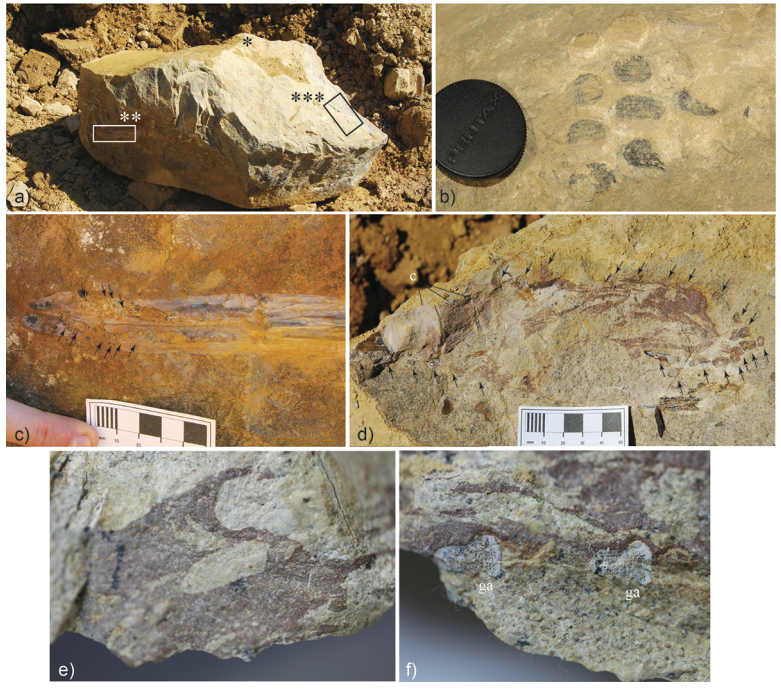




5 cm







Sheet1

Locality	Taxa
Strawberry Bank, Ilminster, Somerset, UK	<i>Stenopterygius triscissus</i> , <i>Hauffiopteryx typicus</i>
Whitby, Yorkshire, UK	various ichthyosaur species
Schistes de Grandcourt, Belgium and Luxembourg	<i>Stenopterygius</i> sp.
Sainte-Colombe, Burgundy, France	<i>Temnodontosaurus burgundiae</i>
Curcy-sur-Orne, Normandy, France	? <i>Stenopterygius</i>
Holzmaden area, Baden-Württemberg, Germany	<i>Temnodontosaurus</i> , <i>Stenopterygius</i> , <i>Hauffiopteryx</i>
Dotternhausen-Dormettingen, Baden-Württemberg, Germany	<i>Hauffiopteryx altera</i> , <i>Stenopterygius</i> sp.
Dobbertin and Grimmen, Mecklenburg-West Pomerania, Germany	<i>Stenopterygius</i> sp.
Staffelegg, Canton Aargau, Switzerland	<i>Eurhinosaurus longirostris</i>
Belmont, Beaujolais, France	<i>Stenopterygius</i> sp.

Table 1. List of early Toarcian localities with ichthyosaur-bearing carbonate concretions (AZ = Ammonite Zo

Sheet1

Stratigraphy

exaratum subzone, *serpentinum* AZ
?

exaratum subzone, *serpentinum* AZ
?*serpentinum* AZ

serpentinum AZ

Base of *serpentinum* AZ (eII4-II6)

Base of *serpentinum* AZ (eII4)

Elegantulum subzone, *serpentinum* AZ
bifrons or *variabilis* AZ

Base of *serpentinum* AZ

Stratigraphic Correlation

post T-OAE

T-OAE not constrained

T-OAE not constrained

T-OAE not constrained

T-OAE not constrained

T-OAE and post-T-OAE

within T-OAE

T-OAE not constrained

post T-OAE

within T-OAE

References

Williams et al. 2015

Benton and Taylor, 1984

Godefroit, 1994

Gaudry, 1892

Dechaseaux, 1954; Mazin, 1988

Böttcher, 1989; Keller 1992

Jäger, 2005, Keller 1992

Maisch & Ansorge, 2004, Stumpf, 2016

Reisdorf et al. 2011

this study

ne)

Lafarge Beaujolais

sample ID	Preservation	Composite height (m)	CaCO ₃ (wt. %)	TOC carb. free IRMS (wt. %)	SD	TOC (wt.%) IRMS	$\delta^{13}\text{C}_{\text{TOC}}$ (‰VPDB)	SD
PL-2013-1	Non-weathered	0.28	1.14	14.46	0.06	14.29	-31.67	0.05
PL-2013-2	Non-weathered	0.30	1.18	13.63	0.56	13.47	-32.05	0.05
DV01-2	Non-weathered	0.42	0.32	12.63		12.59	-31.40	0.01
DV02-2	Non-weathered	0.44	78.57	10.00		2.14	-30.35	
DV03-2	Non-weathered	0.46	69.34	8.94		2.74	-30.88	
DV04-2	Non-weathered	0.48	57.69	10.90		4.61	-30.30	
DV05-2	Non-weathered	0.51	79.26	10.89		2.26	-29.94	
DV06-2	Non-weathered	0.57	57.72	10.27	0.42	4.34	-30.06	0.03
DV07-2	Non-weathered	0.61	11.26	14.78		13.12	-29.59	
DV08-2	Non-weathered	0.64	15.47	13.65		11.54	-29.86	
DV09-2	Non-weathered	0.69	24.74	13.83		10.41	-30.14	
DV10-2	Non-weathered	0.75	1.29	10.21		10.07	-31.40	
DV11-2	Non-weathered	0.81	26.65	9.22		6.76	-29.93	
DV12-2	Non-weathered	0.85	27.81	12.55	0.28	9.06	-29.73	0.03
DV13-2	Non-weathered	0.92	54.43	16.92		7.71	-29.66	
DV14-2	Non-weathered	0.96	89.73	15.68		1.61	-29.66	
L 03	Non-weathered	2.90	27.37	3.42		2.48	-28.39	
L 04	Non-weathered	3.00	29.00	3.08		2.19	-28.93	
L 05	Non-weathered	3.10	31.75	2.89		1.97	-28.80	
L 06	Non-weathered	3.20	32.21	9.56		6.48	-28.85	
L 07	Non-weathered	3.40	43.68	9.67		5.45	-28.98	
L 08	Non-weathered	3.50	35.06					
L 09	Non-weathered	3.60	35.90	9.44		6.05	-29.09	
BB2-NW	Non-weathered	3.65	31.00	8.88		6.13	-28.80	
L 10	Non-weathered	3.70	39.37	10.33		6.26	-28.95	
MA-2013NW	Non-weathered	3.75	50.94	9.52		4.67	-28.51	
L 11	Non-weathered	3.80	53.13	10.41		4.88	-28.68	
L 12	Non-weathered	3.90	37.27	10.48		6.58	-28.54	
L 13	Non-weathered	4.00	30.34					
L 14	Non-weathered	4.10	26.06	12.18		9.01	-28.31	
L 15	Non-weathered	4.20	28.20					
L 16	Non-weathered	4.30	29.17	10.25		7.26	-28.43	
L 18	Non-weathered	4.50	29.75	9.74		6.84	-28.22	
L 19	Non-weathered	4.60	26.47	9.55		7.02	-28.62	
UAB-NW	Non-weathered	5.25	22.00	6.17		4.81	-28.20	
CHI-01	Weathered	0.00	60.43					
CHI-02	Weathered	0.06	68.56					
CHI-03	Weathered	0.11	58.53					
CHI-04	Weathered	0.16	4.74					
CHI-05	Weathered	0.20	4.26					
CHI-06	Weathered	0.23	17.93					
CHI-07	Weathered	0.26	8.93					
CHI-08	Weathered	0.30	28.60					
CHI-09	Weathered	0.35	14.83					
CHI-10	Weathered	0.40	26.24					
CHI-11	Weathered	0.47	73.12					
CHI-12	Weathered	0.53	75.49					
CHI-13	Weathered	0.62	8.19					
CHI-14	Weathered	0.70	12.37					
CHI-15	Weathered	0.78	12.58					

CHI-16	Weathered	0.84	69.55					
CHI-17	Weathered	0.92	93.60					
CHI-18	Weathered	1.10	86.84					
CHI-19	Weathered	1.30	89.53					
CHI-20	Weathered	1.40	27.09					
CHI-21	Weathered	1.54	84.63					
CHI-22	Weathered	1.68	29.11					
CHI-23	Weathered	1.77	82.41					
BB2-W	Weathered	3.65	28.00	0.14		0.10	-24.80	
UAB-W	Weathered	5.25	22.00	0.26		0.20	-25.40	
LI 01	Weathered	0.02	79.89	0.23		0.05	-25.51	
LI 02	Weathered	0.53	72.93	0.29		0.08	-28.20	
LI 04	Weathered	0.88	78.43	0.38		0.08	-29.55	
LI 05	Weathered	1.20	84.27					
LI 06	Weathered	1.62	83.96	1.84		0.30	-27.50	
LI 07	Weathered	1.98	90.84					
LI 08	Weathered	2.11	85.23					
LI 09	Weathered	2.26	89.45	0.77		0.08	-27.02	
LI 10	Weathered	2.61	93.12	1.19		0.08	-27.09	
Nodule 2012	Weathered							

CH11-224	Belemnite	0.02						
Ch09-023	Belemnite	1.83						
CH09-003	Belemnite	3.64						
BLH 01	Belemnite	5.61						
BLH 13	Belemnite	7.85						

$\delta^{13}\text{C}_{\text{carb}}$ (‰VPDB)	$\delta^{18}\text{O}_{\text{carb}}$ (‰VPDB)	$^{87}\text{Sr}/^{86}\text{Sr}$	year of collection	Source
			2013	This study
			2013	This study
			2013	This study
-2.54	-4.75		2013	This study
0.07	-3.44		2013	This study
-1.08	-4.04		2013	This study
1.06	-2.56		2013	This study
-0.89	-3.35		2013	This study
-1.44	-5.51		2013	This study
-0.81	-5.70		2013	This study
-0.90	-5.18		2013	This study
			2013	This study
-0.50	-5.13		2013	This study
-0.82	-5.47		2013	This study
-0.61	-5.04		2013	This study
0.96	-2.90		2013	This study
-0.42	-5.10		2009	Suan et al. (2013)
-0.70	-4.98		2009	Suan et al. (2013)
0.30	-5.14		2009	Suan et al. (2013)
0.48	-5.10		2009	Suan et al. (2013)
0.14	-4.76		2009	Suan et al. (2013)
0.21	-5.01		2009	Suan et al. (2013)
-0.15	-4.83		2009	Suan et al. (2013)
			2010	Suan et al. (2013)
-0.42	-4.82		2009	Suan et al. (2013)
			2013	This study
-0.42	-4.58		2009	Suan et al. (2013)
-2.36	-5.50		2009	Suan et al. (2013)
-1.63	-5.01		2009	Suan et al. (2013)
0.12	-5.11		2009	Suan et al. (2013)
0.23	-5.18		2009	Suan et al. (2013)
0.07	-5.05		2009	Suan et al. (2013)
-0.57	-5.02		2009	Suan et al. (2013)
-0.82	-5.14		2009	Suan et al. (2013)
			2010	Suan et al. (2013)
-3.08	-4.97		2011	This study
-2.95	-5.10		2011	This study
-2.05	-4.75		2011	This study
-2.98	-7.11		2011	This study
-3.15	-9.25		2011	This study
-4.32	-6.94		2011	This study
-4.05	-6.42		2011	This study
-5.45	-5.30		2011	This study
-3.28	-5.79		2011	This study
-4.54	-5.77		2011	This study
-3.31	-4.34		2011	This study
-1.97	-4.89		2011	This study
-2.19	-9.42		2011	This study
-2.09	-5.50		2011	This study
-1.46	-6.10		2011	This study

-2.60	-4.36		2011	This study
-3.00	-4.37		2011	This study
-1.88	-3.34		2011	This study
-3.02	-4.16		2011	This study
-1.87	-4.57		2011	This study
-1.15	-3.23		2011	This study
-1.80	-5.53		2011	This study
-1.21	-3.11		2011	This study
			2010	Suan et al. (2013)
			2010	Suan et al. (2013)
-0.18	-4.90		2009	Suan et al. (2013)
-3.60	-3.89		2009	Suan et al. (2013)
-2.83	-4.00		2009	Suan et al. (2013)
0.96	-2.50		2009	This study
-1.49	-3.27		2009	Suan et al. (2013)
-1.19	-3.08		2009	Suan et al. (2013)
-1.25	-4.48		2009	Suan et al. (2013)
-0.80	-2.40		2009	Suan et al. (2013)
-1.85	-2.23		2009	Suan et al. (2013)
-3.88	-4.18		2012	This study
		0.7071010	2011	This study
		0.7071948	2009	This study
		0.7071911	2009	This study
		0.7072229	2011	This study
		0.7072272	2011	This study